

Unmanned aerial vehicle-based computer vision for structural vibration measurement and condition assessment: A concise survey



Kai Zhou ^{a,*}, Zequn Wang ^a, Yi-Qing Ni ^b, Yang Zhang ^c, Jiong Tang ^c

^a Department of Mechanical Engineering and Engineering Mechanics, Michigan Technological University, USA

^b Department of Civil and Environmental Engineering, The Hong Kong Polytechnic University, Hong Kong, China

^c Department of Mechanical Engineering, University of Connecticut, USA

ARTICLE INFO

Keywords:

Unmanned aerial vehicles (UAVs)
Vibration measurement
Condition assessment
Camera systems
Computer vision

ABSTRACT

With the rapid advance in camera sensor technology, the acquisition of high-resolution images or videos has become extremely convenient and cost-effective. Computer vision that extracts semantic knowledge directly from digital images or videos, offers a promising solution for non-contact and full-field structural vibration measurement and condition assessment. Unmanned aerial vehicles (UAVs), also known as flying robots or drones, are being actively developed to suit a wide range of applications. Taking advantage of its excellent mobility and flexibility, camera-equipped UAV systems can facilitate the use of computer vision, thus enhancing the capacity of the structural condition assessment. The current article aims to provide a concise survey of the recent progress and applications of UAV-based computer vision in the field of structural dynamics. The different aspects to be discussed include the UAV system design and algorithmic development in computer vision. The main challenges, future trends, and opportunities to advance the technology and close the gap between research and practice will also be stated.

1. Introduction

One of the important applications in the field of structural dynamics is structural health monitoring (SHM), which aims at assessing the structural condition, reliability, and integrity through the measurement by sensors, mostly accelerometers and strain gauges. For example, the change in modal properties, such as natural frequencies, mode shapes and their curvatures, and modal strain energy, can be used to indicate the damage occurrence (Shi et al., 1998; Qiao et al., 2007; Xia et al., 2002; Hou et al., 2018). Smart materials offer another sensing mechanism for effective damage detection. Among them, the piezoelectric transducer (PZT), which is based upon self-sensing interrogation, has exhibited its high sensitivity in detecting the electromechanical behavior change caused by small-sized damage (Cao et al., 2023; Fan et al., 2018; Shuai et al., 2017; Wang et al., 2013). Shape memory alloy, as another typical smart materials, has also been successfully embedded into structures for damage detection purposes (Bielefeldt et al., 2018; Davis et al., 2021). Despite the success of damage detection using the above sensors, their wide deployment in realistic engineering structures is hindered by several reasons. First, each individual sensor that is physically attached

on the structure only allows the single-point measurement. To acquire sufficient measurements for effective damage detection, many contact sensors are required to distribute over the entire structure, leading to the cumbersome sensor installation and placement of data acquisition (DAQ) system (Feng and Feng, 2018). Second, the adverse effect of incorporating many contact sensors is the additional weight induced (i.e., unrealistic loading), which alters the dynamic characteristics of the structure, thereby resulting in the negative interference in damage detection (Havarani and Mahmoudi, 2020). Finally, the sensor placement becomes essential to ensure the desired damage detection performance, which requires extra investigation (Zhou et al., 2017; Zhou and Wu, 2017; Wu et al., 2019a).

To address the above shortcomings of conventional sensing techniques, significant efforts have been made to develop non-contact full-field sensing techniques for SHM. By utilizing the laser doppler effect due to the structural motion, the scanning laser doppler vibrometer (SLDV) is able to continuously scan the measurement points over the surface of a sinusoidal excited structure, enabling the full-field vibration measurement (Stanbridge and Ewins, 1999). Noteworthy, SLDV can also be used to conduct the experimental wave propagation analysis, which directly

* Corresponding author.

E-mail addresses: kzhou@mtu.edu (K. Zhou), zequnw@mtu.edu (Z. Wang), ceyqni@polyu.edu.hk (Y.-Q. Ni), yang.3.zhang@uconn.edu (Y. Zhang), jiong.tang@uconn.edu (J. Tang).

facilitates damage detection. Specifically, the high-frequency wave, i.e., ultrasonic wave can be excited and propagated through the entire structure to construct the wavefield. The wavefield contains the wave propagation characteristics with respect to the time, from which the suspicious damage can be localized when a sudden change of the wave propagation characteristics is observed (Kudela et al., 2017; Maio et al., 2018; Pieczonka et al., 2017). While SLDV has been well established as a valuable instrument for nondestructive testing (NDT) in the structural dynamics community, SLDV has some notable drawbacks. SLDV requires a long testing time because it measures all of the discrete points on the structure *sequentially* rather than *concurrently* (Reu et al., 2017). SLDV usually is placed close to the target/object, which makes it ineffective for large-scale and inaccessible engineering structures, such as offshore wind turbines. Besides, SLDV is expensive and bulky, which is not suited to actual implementation scenarios (Maio et al., 2018).

As a relatively new technology, machine vision-based sensing well overcomes the disadvantages of SLDV and thus shows a promising prospect in vibration measurement. Machine vision-based sensing generally refers to the high-speed camera-based image and video recording. The key aspect of this sensing technique is image processing, which directly analyzes the images and then extracts the vibrations. Over the past decade, various image processing techniques have been developed to empower machine vision-based sensing. A technique so called phase-based motion magnification can be applied to a series of motion frames/images in a video from the high-speed camera to quantify the full state of motion of a structure/system. This technique has been successfully employed for structures/systems in various industries (Eitner et al., 2021; Sarrafi et al., 2018; Chen et al., 2018; Poozesh et al., 2017). Additionally, digital image correlation (DIC) has become mainstream in image processing for vibration measurement (Trebună and Hagara, 2014; Huñady et al., 2019; Beberniss and Ehrhardt, 2017; Helfrick et al., 2011). A stereo camera setup is required to implement the DIC analysis. A stereo camera has two or more lens, which is designed to mimic human binocular vision. The images recorded from the different lens can be used to estimate the 3-dimensional coordinates of points on a target/object via the so-called photogrammetry, thus realizing the vibration measurement (Niezrecki et al., 2010). As a target-based method, the artificial speckle pattern needs to be mounted on the target to ensure the robustness of the measurement (Helfrick et al., 2011). In contrast to the target-based method, the targetless approaches, such as edge detection and tracking technique and its variants, have also been widely used for vibration measurement (Bai et al., 2020a; Javed et al., 2022). The sufficient vibration information from the full-field measurement significantly benefits the subsequent model updating procedures for structural damage identification (Zhou and Tang, 2021a, 2021b; Weng et al., 2011; Adeagbo et al., 2021; Wang et al., 2018; Hua et al., 2008).

Noteworthy, the images already contain detailed information on the structure surface. In other words, the defect on the structure surface is visible in nature, which allows direct detection without the intermediate step on vibration measurement as mentioned above. Thanks to the advent of deep learning, especially in computer vision, direct damage detection based on the image becomes entirely possible. In recent years, deep learning enabled computer vision has seen a surge of interest because of its power to directly interpret images. Deep learning methods have been continuously developed and enhanced in order to broaden the applications in diverse scientific disciplines. From the machine learning perspective, damage detection using computer vision, fundamentally belongs to either the object detection, image classification, or segmentation task (Deng et al., 2020; Zhang et al., 2020a; Huang et al., 2020). Depending on the image quality, image preprocessing becomes one favorable option prior to implementing the computer vision. For example, image denoising and image deblurring are the most commonly adopted image preprocessing procedures (Wang and Tao, 2014; Fan et al., 2019). Using the fixed camera system for image acquisition followed by computer vision for damage detection has been reported in several studies (Huang et al., 2020; Li et al., 2019; Cha et al., 2017).

The dynamic camera systems have evolved along with the rapid development of robotic technology. It is evident that the dynamic camera systems offer great mobility during image acquisition, which are superior to the fixed camera system. There are various types of dynamic camera systems that have been purposely designed to fulfill different missions. For example, inspection vehicle (Nagaya et al., 2012; Ekkachai et al., 2022; Nakamura et al., 2019) and climbing robot (Jang et al., 2021; Nguyen and La, 2019, 2021; Wang et al., 2017) have been found with effectiveness in conducting the inspection tasks. UAV, also known as drone, on the other hand, is a prominent technique to carry the portable cameras for remote sensing purposes. Compared to the fixed and other dynamic camera systems, UAV has excellent mobility and wide area coverage, which ensures its good accessibility to remote engineering structures. Furthermore, UAV can essentially be deemed an advanced camera system, which is subject to secondary development/design to suit broad applications. To the best of our knowledge, such system redesign generally involves hardware development including but not limited to 1). Different types of cameras can be installed on the UAV with real-time information exchange; 2). Onboard computing unit, i.e., CPU can be installed on the UAV, leading to the computer vision enabled UAV, which can further leverage the Internet of Things (IoT) technology to advance SHM capacity. 3). Control system can be embedded into the UAV to guide/manage the UAV flight trajectory to adapt to the missions under different weather conditions. By appropriately designing the flight trajectory, the images can be captured from the entire angular field of view, which are used to construct the virtual reality (VR) and augmented reality (AR) environments. For these reasons, UAV-based vision can be tailored for a broad range of applications, including but not limited to the injury surveillance/monitoring/detection, safety assessment in the emergency situations and hazard events, traffic flow estimation and highway infrastructure management, etc (Andriluka et al., 2010; Brunetti et al., 2018; Khan et al., 2020; Allouch et al., 2019; Zacharie et al., 2018; Outay et al., 2020).

It is noted that UAV-based vision recently has become a trending technology for remote vibration measurement and structural damage detection. Using the search keywords [“vibration measurement” or “damage detection” and “unmanned aerial vehicle”] within Scopus database, the number of articles over the past few years is identified and shown in Fig. 1. The chart clearly indicates the rapid growth of recent interest in this research topic and relevant progresses that have been achieved. Khadka et al. proposed a robust practice for wind turbine monitoring by utilizing a DIC system with the UAV as a mainstay. A laboratory testing on a scale-down wind turbine system was carried out to validate the method (Khadka et al., 2020). Following the similar idea, Chen et al. applied this method onto bridge vibration measurement (Chen et al., 2018).

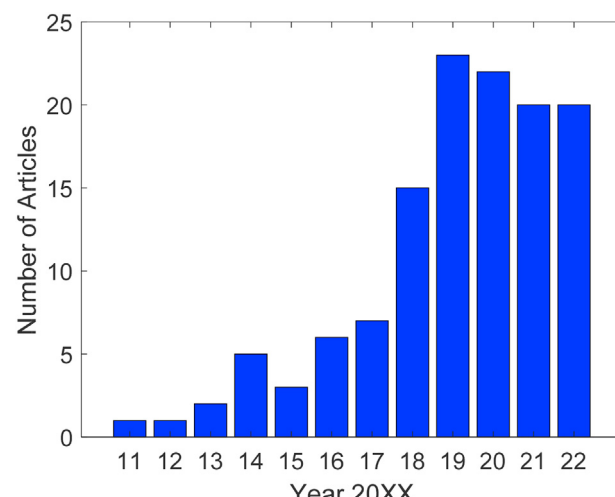


Fig. 1. Research outcome over the years according to Scopus database.

2021). Hallermann and Morgenthal used UAV for the visual inspection of large bridges, which was a pilot study to prove the computer vision concept for automatic damage detection (Hallermann and Morgenthal, 2014). Wang et al. developed a graphics-based digital twin (GBDT) framework that is built upon the physical FE modeling and computer vision for post-earthquake structural inspection and evaluation. The effectiveness of the framework is validated by the UAV-based inspection on a five-story reinforced concrete benchmark building (Wang et al., 2022a). As will be shown later, more literature will be systematically reviewed and discussed in terms of various aspects ranging from hardware configuration, and algorithmic development to application. This article will also discuss the current challenges of UAV-based applications in structural dynamics and point out the potential improvements for advancement. Within the context of the UAV applications, this review article will be limited to a narrower scope, compared to the existing review articles, on the computer vision-based structural dynamics (Bao et al., 2019; Xu and Brownjohn, 2018; Dong and Catbas, 2021) and robotics technologies for infrastructure inspection (Lee et al., 2023). This thus makes the unique contribution to research community.

2. UAV system, image acquisition, and preprocessing for quality assurance

UAV products/systems for professional and research use are from a wide range of developers and manufacturers, including *Ascending Technologies*, *Applanix*, *DJI technology*, etc. In addition to the standard UAV products, customized solutions will also be provided by those UAV manufacturers for specific purposes and missions. As shown in Fig. 2, UAV systems can be generally classified into four categories, namely single-rotor UAV, multi-rotor UAV, fixed-wing UAV, and hybrid fixed-wing UAV. According to the number of rotors, multi-rotor UAV can be further classified into *Tricopter*, *Quadcopter*, *Hexacopter*, and *Octocopter*. While the UAV systems can be utilized for a vast variety of applications and can be designed with complete hardware units to accommodate certain challenging tasks, in this section, we only collect information of UAV systems used for structural dynamics applications, with a specific emphasis on the UAV type, and camera model and its key specification.

The details of UAV systems are briefly summarized in Table 1. From the collected literature, the mostly used UAV models are manufactured from the *DJI technology*, and the multi-rotor UAV apparently is a dominant type in applications. The reason may lie in that multi-rotor UAV has good maneuverability, which can hover in place and fly towards different directions without the need to change the orientation. Among all multi-rotor UAV types, *Quadcopter* appears to be the most popular one as it has relatively small weight and low cost compared to *Hexacopter* and *Octocopter*. Moreover, one may notice that dual cameras are installed in some UAVs, the intention of which is to form a stereo camera system to facilitate photogrammetry. This will be introduced in detail later.

Once the image acquisition using the UAV camera system is complete, an image preprocessing procedure is preferably carried out to ensure good-quality images for the sake of subsequent analysis. The preprocessing is especially necessary for outdoor image acquisition due to its vulnerability to weather conditions. The selection of image preprocessing methods is case-dependent. Some typical image preprocessing methods include image denoising and filtering, image deblurring, image normalization, and image augmentation. Because of the imperfect instrumentation during the data acquisition, the images are inevitably contaminated by noise. As such, denoising the images is a critical and frequently adopted method of image preprocessing. Research on image denoising technique development has continued over a few decades. Image denoising is implemented by different types of algorithms, ranging from spatial filtering, transform domain filtering to data-driven transform (such as independent component analysis (ICA)) (Ahmadi et al., 2013). In each type of algorithms, linear or nonlinear filters can be employed depending on the collected images. Linear filters usually deal with signal corruption by Gaussian noise in the sense of mean square error. As a representative linear filter, the mean filter smooths the images by reducing the intensity variation between adjacent pixels. It essentially is a sliding window spatial filter that replaces the center value in the window with the average of all the neighboring pixel values (Ahamed et al., 2019). Compared to linear filters, nonlinear filters effectively remove other types of noises that cannot be explicitly represented. A variety of median-type filters have been developed for nonlinear filtering purposes. Given the current pixel being considered, the filtering first sorts

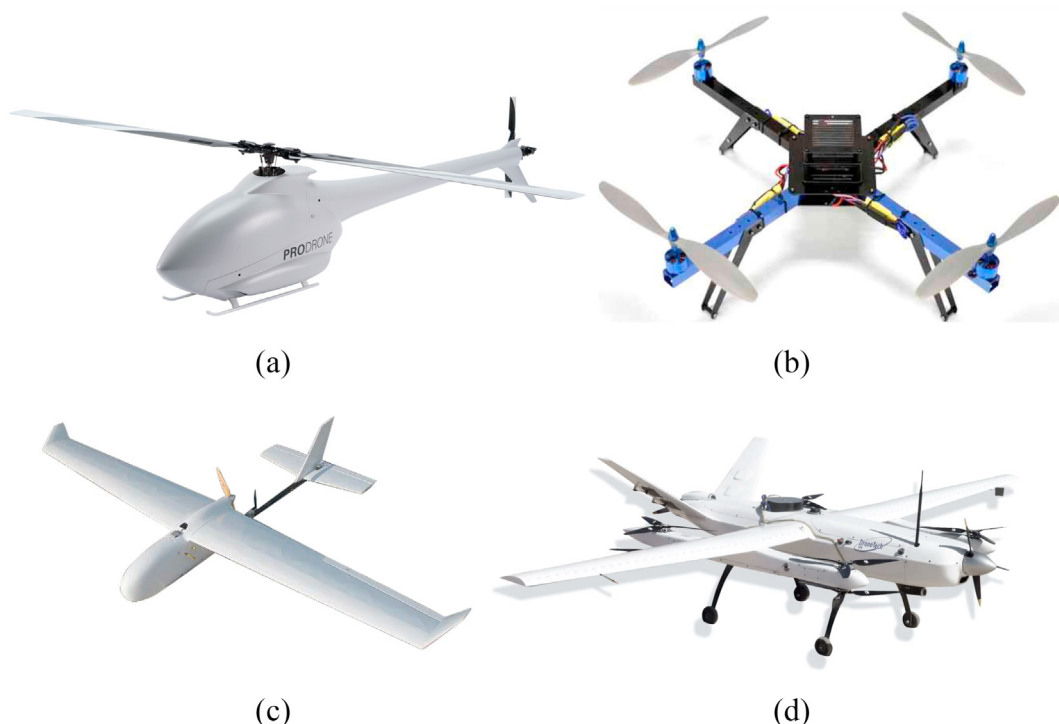


Fig. 2. UAV types (a) single-rotor UAV; (b) multi-rotor UAV; (c) fixed-wing UAV; (d) hybrid fixed-wing UAV.

Table 1

UAV camera systems used in structural dynamics applications.

Reference	UAV Type, (Manufacturer and Model)	Camera and Resolution
Hallermann and Morgenthal (2014)	Multi-rotor UAV, Octocopter (Ascending Technologies: BUW Falcon)	Panasonic Lumix DMC TZ: 14.1 megapixels Sony Nex 5 22: 14.2 megapixels
Khadka et al. (2020, 2022)	Multi-rotor UAV, Octocopter	Two Point Grey GS3-U3-32S4M – C cameras: 3.2 megapixels
Wang et al. (2022b)	Mutli-rotor UAV, Quadcopter (DJI technology: Mavic Pro)	Integrated camera: 12 megapixels
Li et al. (2022a); Xiong et al. (2020)	Mutli-rotor UAV, Quadcopter (DJI technology: Phantom 4 Pro)	Integrated camera: 20 megapixels
Zhang et al. (2017); Pierce et al. (2018)	Multi-rotor UAV, Hexacopter (Ascending Technologies: Firefly)	CM3-U3-50S5CCS camera: 4 megapixels
Rao et al. (2019)	Mutli-rotor UAV, Quadcopter	Integrated camera: 1 megapixel
Zhang et al. (2022)	Mutli-rotor UAV, Quadcopter (DJI technology: Mavic Air 2)	Integrated camera: 12 megapixels
PengLinLiu (2021)	Mutli-rotor UAV, Quadcopter	Integrated miniature camera: 0.24 megapixels
Eschmann et al. (2012)	Mutli-rotor UAV, Octocopter (Mikrokopter MAV platform)	Canon PowerShot SX220 HS: 12 megapixels
Taj et al. (2020)	Mutli-rotor UAV, Quadcopter (DJI technology: Mavic Mini)	Integrated camera: 12 megapixels
Ayele et al. (2020)	Mutli-rotor UAV, Quadcopter (DJI technology: Matrice 100)	Integrated aerial zoom cameras: 12.4 megapixels
Kim et al. (2018)	Mutli-rotor UAV, Quadcopter (DJI technology: Inspire 2)	Zenmuse X5S camera: 15.7 megapixels
Alzarrad et al. (2022)	Mutli-rotor UAV, Quadcopter (DJI technology: Matrice 300 RTK)	Zenmuse H20T camera: 12 megapixels
Santos et al. (2022)	Mutli-rotor UAVs, Quadcopter (DJI technology: Mavic Mini), Octocopter (DJI technology: Matrice 600 Pro)	Integrated camera: 12 megapixels Zenmuse X5 camera: 16 megapixels
Wen and Kang (2014)	Multi-rotor UAV, Hexacopter (DJI technology)	Sony NEX-5R w/ SEL16F28: 16.1 megapixels
Reagan et al. (2017, 2018)	Multi-rotor UAV, Quadcopter (Physical Science, Inc.: InstantEye Gen4)	Integrated cameras: 2 megapixels
La et al. (2019)	Multi-rotor UAV, Octocopter (UAV Systems International: TAROT X8)	Point Grey GS3-U3-32S4M – C camera: 3.2 megapixels
Liu et al. (2022)	Multi-rotor UAV, Quadcopter (DJI technology: Phantom 4 Pro)	Xiaomi 12S Ultra: 50 megapixels Integrated camera: 20 megapixels
Lianpo (2022)	Fixed-wing UAV (Sensefly)	Canon S 110 RGB: 12 megapixels

all the neighboring pixel values with a numerical order and then replaces the current pixel with the *median* pixel value. Such filtering process is mathematically described as

$$\tilde{p}_{i,j} = \text{med}(s(p_{i,j})) \quad (1)$$

where $p_{i,j}$ is the value of pixel at i -th and j -th positions in horizontal and vertical directions of an image, respectively. $\tilde{p}_{i,j}$ is a new pixel value. $s(\cdot)$ denotes the operator to identify all neighboring pixels of $p_{i,j}$. $\text{med}(\cdot)$ is the operator to find the median pixel value.

Since the UAV is fast-moving, the images captured might exhibit significant blurriness, i.e., motion blur. This issue may further be compounded by windy weather. Other different types of blurs also will be induced, such as defocus blur and atmospheric turbulence blur. To identify the cause of image blur, it is necessary to look into the imaging process, which generally can be formulated as (Wang and Tao, 2014)

$$y = f(x^*h) + n \quad (2)$$

where x is the latent sharp image from the geometric operator, and h is the approximated blur kernel. $f(\cdot)$ denotes the nonlinear camera response function. n denotes the noise. For simplification, the linear camera response is considered, and Equation (2) can then be re-written as

$$y = x^*h + n \quad (3)$$

Given the above equation, the aim of the image deblurring is to recover an accurate x or to recover both x and h (blind deblurring) from the observation y , which fundamentally is an inverse problem to be solved. As can be seen in Equation (3), image deblurring can be treated as a convolution process. Solving the inverse problem hence resorts to the deconvolution technique. Due to its inverse nature, deconvolution can be facilitated by employing widely available optimization algorithms (Wipf and Zhang, 2015; Cai et al., 2018; Tai et al., 2008). It is worth noting that deblurring images may cause noise effects in some scenarios because of the resulting image sharpness, which requires extra investigation to reach a satisfactory compromise/trade-off (Mitra et al., 2014).

Image normalization is a procedure to change the range of pixel intensity values in the image, which establishes a reference for different sets of images taken under various illumination/lighting conditions. This is especially useful for UAV-based image acquisition because the task is executed at the outdoor environment. With the growing demand for UAV-based image acquisition, image normalization has been increasingly adopted (Lu et al., 2011; Yan et al., 2019; Thompson and Puntel, 2020). Different from the image denoising, deblurring, and normalization mentioned above, image augmentation aims to artificially create extra images through the multiple types of operations on the existing images, such as rotation, shift, flip, etc. (Shorten and Khoshgoftaar, 2019). As will be shown later, image augmentation is a necessary step to adequately train a complex deep learning model and minimize the likelihood of model overfitting when the available training dataset is limited.

3. Digital image processing for non-contact and full-field vibration measurement

Digital image processing is a dispersible part of computer vision, which is found to be a prominent tool for extracting dynamic vibrations from images or videos. It is important to note that the concept of *image processing* differs from that of *image preprocessing* mentioned previously. Image preprocessing is closely relevant to image clean-up for quality improvement, while image processing tends to utilize complex transformation to retrieve useful information which cannot be visually obtained from the images.

Many different methods have been developed thanks to continuous and extensive image processing research. One important class of image processing methods is the so-called digital image correlation (DIC). DIC uses two cameras, i.e., a stereo pair of cameras to establish the binocular vision for in-plane and out-of-plane displacement measurements (i.e., 3-dimensional measurement) based on the theory of photogrammetry. DIC first builds the mapping relations between the image coordinates of the right camera and real space coordinates and between the image coordinates of the left camera and real space coordinates. Then, the real space coordinates can be computed from the constraint associated with the overlapping coordinates of the target points in both images. Fig. 3 shows the schematic to calculate the coordinates, i.e., $[X_W, Y_W, Z_W]$ in the real space based upon the coordinates of the target points using the binocular vision based DIC. Detailed mathematical derivations can be found in (Wang et al., 2019) for interested audiences. As can be observed, the target points are required to implement the DIC analysis, and the structure may not have the texture features to be used as target points. The additional set of artificial target points, such as speckle patterns and optical targets, hence, need to be placed on the structure. Overall, the DIC method is very robust, enabling a wide range of applications in multiple

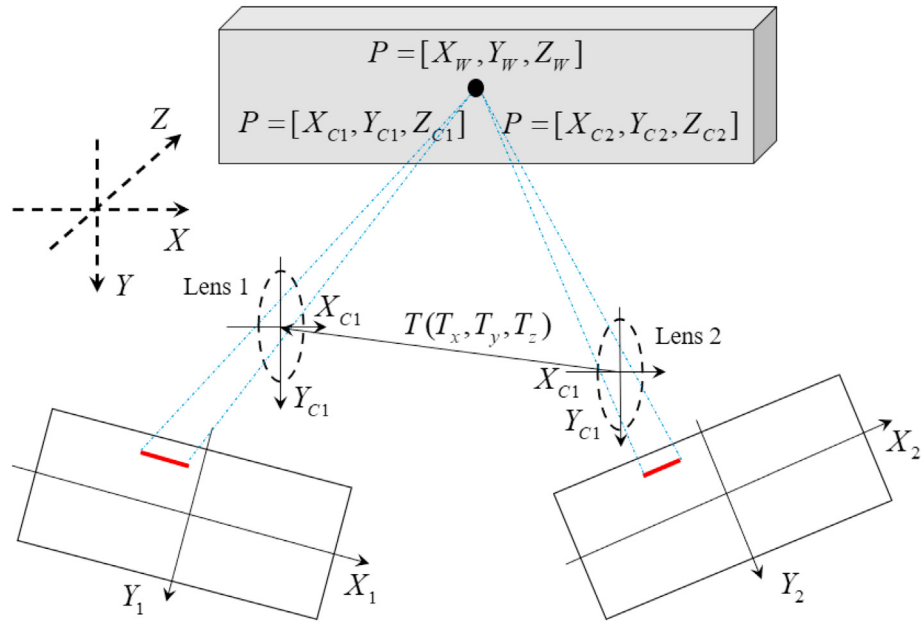


Fig. 3. Schematic of binocular vision-based DIC. Adapted with permission from (Wang et al., 2019).

areas (Helfrick et al., 2011; Gencturk et al., 2014; Pan et al., 2009; Sanz et al., 2010). Point tracking (PT) is another representative method for target-based image processing. The target centers are detected using an ellipse search algorithm, and the coordinates of the points in the real space are then identified using triangulation. Three-dimensional point tracking (3DPT) computes the displacement of the targets by tracking them in different time stages and comparing their coordinates with the reference stage. The artificial target points mounted on the structure using PT usually is larger than that using DIC (Baqersad et al., 2017).

Other methods have also been developed to meet the increasing needs of image processing. In contrast to the target-based methods, the targetless methods search for the illumination change or defined shapes in the structure and thus do not need speckle patterns attached (Ferrer et al., 2015). In other words, the targetless methods use the existing geometry features of the structure as the targets. The most common targetless methods include edge detection, pattern matching, and blob detection methods (Baqersad et al., 2017). Among them, edge detection methods are most frequently used. As will be shown in the subsequent section, edge detection methods have also been used to directly identify and quantify the damage from the image. While the targetless methods can be implemented without placing the extra artificial target and generally feature less computational complexity than the target-based methods, their notable drawback is the inferior accuracy and robustness compared to the target-based methods, especially when the images are unclear and have bad intensity contrast between the background and structure. This causes the internal features difficult to be tracked.

Recently, new image processing techniques, collectively called motion magnification were introduced to magnify the small motions in the camera-captured videos (can be treated as a series of sequential images/frames) for vibration measurement. The basic principle behind motion magnification is to obtain a representation of the video in which the signals representing the motions of the structure can be time-frequency bandpass filtered, and amplified. With this, a new motion magnified video will be reconstructed (Shao et al., 2022; Chen et al., 2015). The phase-based motion magnification originally proposed by (Wadhwa et al., 2013), and its variants have been popularly adopted. This technique decomposes each signal/image of a video into spatially structured images of different scales and orientations using complex-valued steerable pyramid filters (Shao et al., 2022). The phase signals at each

location, orientation, and scale then are temporally bandpass filtered, amplified, and reconstructed. The entire process workflow is provided by (Chen et al., 2015), shown in Fig. 4. Compared to the abovementioned methods, phase-based motion magnification can ensure a high signal-to-noise ratio (SNR) at high frequencies, leading to the enhanced accuracy of the high-frequency vibration measurement.

The template matching method tends to move the template over the entire image and evaluate the similarity between the template and the sliding window in the image. This process can be mathematically represented as a two-dimensional convolution (Kerwin, 2009). The general metric for similarity measurement is the normalized correlation coefficient (NCC), which is expressed as (Han et al., 2022)

$$R(x, y) = \sum_{x', y'} (T'(x, y) * I'(x + x', y + y')) \quad (4)$$

where T' and I' denote the image and template, respectively, after normalization through

$$T'(x, y) = \frac{T(x, y) - \frac{1}{w \times h} \sum_{x', y'} T(x', y')}{\sqrt{\sum_{x', y'} T(x', y')^2}} \quad (5a)$$

$$I'(x, y) = \frac{I(x, y) - \frac{1}{w \times h} \sum_{x', y'} I(x', y')}{\sqrt{\sum_{x', y'} I(x', y')^2}} \quad (5b)$$

There are other available metrics for the matching function, such as the sum of squared difference (SSD) (Hisham et al., 2015) and orientation code matching (OCM) (Ullah and Kaneko, 2004).

The rapidly growing demand of using image processing for diverse applications boosts the releases of some photogrammetry software, such as *ContextCapture* (developed by Bentley Systems), *PONTOS™* (developed by GOM) to facilitate the project implementation. Due to the increasing utilization of UAV for image acquisition in recent years, digital image processing methods have started with applications for vibration measurement. It, however, is worth mentioning that some methods, such as phase-based motion magnification, only have been employed using the stationary high-speed camera instead of the UAV-based camera

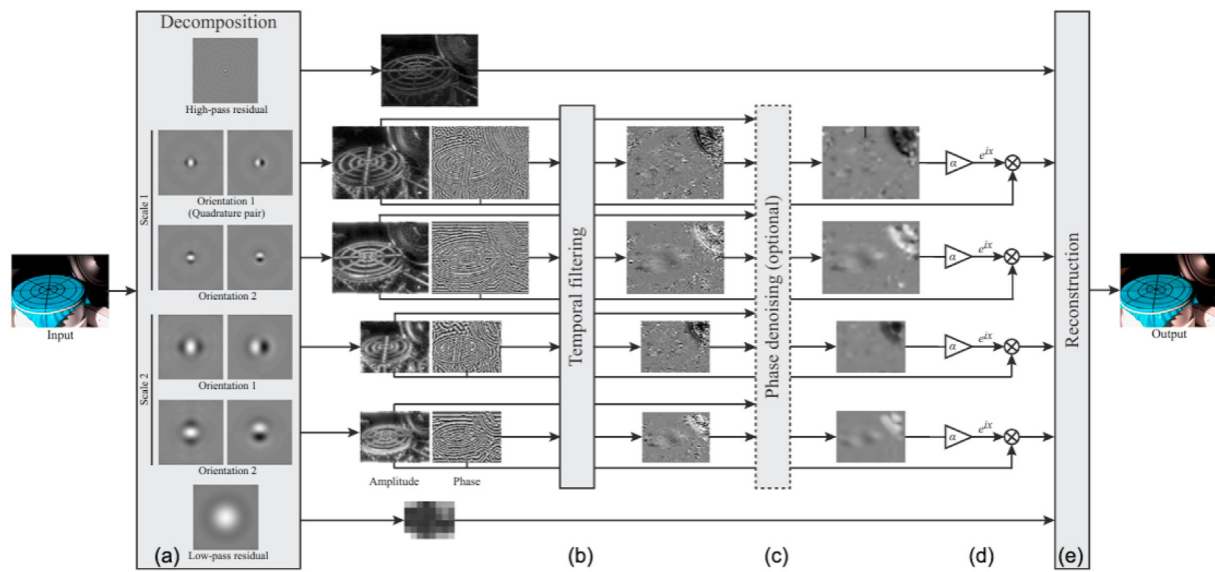


Fig. 4. Workflow of phase-based motion magnification (a) complex steerable pyramid filters decompose the video into the amplitude and phase at different scales; (b) decomposed phases are bandpass filtered in frequency; (c) amplitude-weighted smoothing is applied; (d) bandpassed phases are amplified; (e) new video is reconstructed. Reprinted with permission from (Chen et al., 2015).

system (Sarrafi et al., 2018; Yang et al., 2017; Peng et al., 2020; An and Il Lee, 2022). The relevant studies are summarized in Table 2.

4. Computer vision for structural condition assessment

The vibration measured is the key information for inverse model updating-based structural condition assessment. While the inverse model updating that is built upon a physical baseline model appears to be a well-established methodology, it is challenging to construct a high-fidelity physical model for certain complex scenarios and to incorporate the entire image pixels directly into the updating process. As a result, there are rare studies that fall into this specific topic. Computer vision, on the other hand, is tailored to UAV image-based damage detection because it intends to gain a high-level understanding of the damage related features of digital images. This section hence will comprehensively review and

discuss the state of the art that utilizes the computer vision techniques for structural condition assessment. It is worth pointing out that for accurate damage size estimation, i.e., 3-dimensional (3D) damage quantification, 3D vision sensor that is comprised of stereo setup of multiple 2D vision sensors usually is adopted to facilitate the implementation of the computer vision techniques (Yuan et al., 2022). In general, computer vision techniques for damage detection consist of two folders, i.e., image processing and machine learning.

4.1. Image processing in computer vision for damage detection

Given the premise that the RGB values of pixels in damage differ from that in the image background, image processing is expected to detect, locate damage, and then quantify the damage size by analyzing the image pixels. Some image processing methods for vibration measurement

Table 2

Summary of the state-of-the-art image processing methods for UAV-based vibration measurement.

Method	Description	Application
Digital image correlation (DIC) and 3D point tracking (PT)		Lab-scale truss bridge vibration measurement (Chen et al., 2021; Wu et al., 2021; Zhang et al., 2021); scaled-down wind turbine blade vibration measurement (Khadka et al., 2020, 2022); infield vibration measurement of an actual wind turbine (Ozbek et al., 2010); vibration measurement of a supported wooden beam (Lin et al., 2022); vibration measurement of a scaled bridge girder and an actual bridge deck (Kumarapu et al., 2022); vibration measurement of two in-service concrete bridges (Reagan et al., 2018); displacement measurement of landslide (Liando, 2022); vibration measurement of an infrastructure system (Report and Bas, 2022)
Edge detection and its variants		Tower-swaying displacement measurement (Khuc et al., 2020); detection of motion of the objects in aerial images (Cu et al., 2018); vibration detection of the buildings and streets (Afolabi et al., 2015)
Template matching and its variants		Vibration measurement of a lab-scale two-story shear frame and an actual bridge (Han et al., 2022); vibration measurement of a multiple-purpose testing system (MTS) (Bai and Yang, 2021); deformation measurement of an ancient tower (Ye et al., 2021)
Other methods	Homograph transformation	Displacement measurement of a lab-scale six-story shear-building model and an actual elevator tower (Weng et al., 2021)
	Heuristic image processing with numerical integration	Displacement measurement of a target fixed to a massive reinforced concrete (RC) wall (Ribeiro et al., 2021)
	Target identification with direct linear transformation (DLT)	Vibration measurement of cantilever plate in the laboratory (Perry and Guo, 2021)
	Image-to-point cloud conversion followed by the optimization algorithm to identify the fitting plane	Vibration measurement of a numerical building model (Sun et al., 2022)
	A framework consists of sequential steps: optimal imaging, local feature extraction, optimal matching, and a combined adjustment	Displacement measurement of the soil nail walls (Esmaeili et al., 2019)
	Convolutional neural networks (CNNs) with Kanade–Lucas–Tomasi (KLT) optical-flow method	Lab-scale truss bridge vibration measurement (Yan et al., 2022)

(introduced in Section 3) can be extended for direct damage detection following the same principle. Among those methods, the edge detection method that identifies the points in an image with discontinuities, i.e., sharp changes in image brightness, plays a predominant role. These points where the image brightness varies sharply are defined as edges of the image (Dhankhar and Sahu, 2013). Some commonly used edge detectors include Sobel edge detectors, Canny edge detectors, Prewitt edge detectors, and Laplacian edge detectors. The Sobel edge detector is built upon the spatial gradient algorithm that can detect the gradient, i.e., change in image intensity. The image is convolved with a Sobel mask, resulting in the first-order partial derivatives. Two convolution masks with size 3×3 usually are adopted to compute the derivatives in both x and y directions of the image. They are described as (Abdel-Qader et al., 2003)

$$\mathbf{M}_x = \begin{bmatrix} 1 & 2 & 1 \\ 0 & 0 & 0 \\ -1 & -2 & -1 \end{bmatrix} \quad \mathbf{M}_y = \begin{bmatrix} -1 & 0 & 1 \\ -2 & 0 & 2 \\ -1 & 0 & 1 \end{bmatrix} \quad (6)$$

While the Canny edge detector also is a convolution filter, it is slightly more powerful than the Sobel edge detector. When using Canny edge detector, an image is first smoothed by convolving with a Gaussian mask to eliminate the noise. The edges then are detected at the maxima of the gradient. Following these procedures, this detector can generate an edge strength and direction at each pixel in the smoothed image. Because of their simplicity and effectiveness, edge detection methods have been employed for processing UAV images and thus facilitate damage detection of different engineering structures, for example, concrete bridge monitoring (Yu et al., 2017), road damage detection (Nappo et al., 2020; Sui et al., 2014), and building crack inspection (Choi and Kim, 2015).

Some transform methods that originally were intended for signal processing analysis, e.g., fast Fourier transform (FFT) and fast Haar transform (FHT), have also been proven effective in processing UAV-taken images for damage detection (Abdel-Qader et al., 2003). In the context of imaging processing, FFT is an algorithm to characterize the interconversion between the spatial domain representation and the frequency domain representation of images, while FHT is a relatively new algorithm, decomposing the image into different low-frequency and high-frequency components, followed by the high-frequency component isolation to identify the edge features of an image (Abdel-Qader et al., 2003). Moreover, mathematical morphology (MM) is another powerful algorithm to distinguish various shapes and sizes from the image through time-domain analysis. MM employs set operator to conduct the image transformation by taking their topological and geometric properties into account. The basic morphological set transformations are *erosion* and *dilation*. *Erosion* removes small objects and disconnects objects connected by a small bridge, while *dilation* fills holes and smoothens the contour lines in the image. The main advantage of MM is to preserve the original geometry features of the large objects. As a comparison, the Gaussian mask used to remove the noise in the abovementioned edge detection methods may blur the image. With MM as an image processing tool, UAV images can be appropriately handled to facilitate the condition monitoring tasks (Wu et al., 2020; Oliveira et al., 2018; Galantucci and Fatiguso, 2019). In addition to the above well-established methods, other advanced methods have also been developed to improve image processing capability. Kim et al. developed a hybrid image processing method that performs the hybrid binarization of UAV-taken images for concrete crack estimation while minimizing the loss of other useful information in the image (Kim et al., 2017). Lei et al. developed a new image processing method for crack detection, namely the crack central point method (CCPM), which improves the detection robustness under relatively fuzzy and low-contrast images (Lei et al., 2018). Kakooei and Baleghi established a new framework built upon the building environment and image processing techniques and applied it to UAV oblique images to assess the post-disaster damage. The image datasets collected under different earthquake scenarios were used to comprehensively

verify the methodology (Kakooei and Baleghi, 2017). Continuous development of image processing methods is vital in advancing UAV-based SHM technology.

4.2. Machine learning in computer vision for damage detection

While image processing has demonstrated its feasibility in damage detection, it essentially only facilitates decision making and cannot automate/streamline the whole detection process. To circumvent such issue, machine learning that inherently is built upon data-driven modeling sheds a new light for damage detection. Indeed, some traditional machine learning methods, such as support vector machine (SVM), and K -nearest neighbors (KNN), have been practiced on UAV-based damage detection (Ichi and Dorafshan, 2022; Avola et al., 2021; Chen and Liu, 2021; Zhang et al., 2020b). However, the data preprocessing step, e.g., feature extraction and dimension reduction of UAV-taken images is required to implement those methods. Deep learning, as a new class of machine learning methods, primarily inherits the neural network architecture and can be performed without the data preprocessing. It is well known that the convolutional neural network (CNN) offers a baseline deep learning architecture, based upon which many variants of deep learning neural networks have been developed to broaden the applications with enhanced performance. While numerous studies exploiting deep learning methods can be found, we will particularly be interested in discussing the deep learning methods in the context of UAV-based damage detection and condition assessment.

Some representative studies with significant attention (indicated by the citation number) will be emphasized. Shihavuddin et al. applied a series of deep learning models together with the UAV inspection images to conduct the wind turbine surface damage detection. In this work, four different types of surface conditions including i.e., leading edge (LE) erosion, vortex generator (VG) panel, vortex generator (VG) panel with missing teeth, and lightning receptor are considered in the UAV inspection images (Fig. 5a). Among different models, the model with Inception-ResNet-V2 architecture shows the best damage detection accuracy that was evaluated by *Mean Average Precision* (MAP). The effect of data augmentation on deep learning performance was also investigated. It was found that the data augmentation indeed can serve as the performance multiplier (Shihavuddin et al., 2019). The implementation flowchart of the damage detection is shown in Fig. 5b.

Xiong et al. developed an automated building seismic damage assessment using a UAV and a convolutional neural network (CNN). The 3-D building model was first built for UAV-taken building image segmentation. Treating segmented images and respective damage states (each damage state represents a class) as input and output, respectively, a CNN classifier with VGG-16 transfer learning then was established and the classification accuracy was thoroughly examined. The proposed methodology enables the prediction of the region-based distribution of building seismic damages, which benefits emergency relief (Xiong et al., 2020). The framework of the proposed methodology is shown in Fig. 6. Similarly, Gopalakrishnan et al. proposed to use a pre-trained VGG-16 CNN for crack detection of civil infrastructure based on the UAV-taken images. The deep learning method in this work essentially serves the binary classification task (i.e., crack and intact states). The results show that the proposed method can yield up to 90% accuracy in crack detection in realistic scenarios without any augmentation and preprocessing (Gopalakrishnan et al., 2018).

The extensive studies are discussed in terms of the deep learning method/model details, analysis type, application, and outcome, which are put together in Table 3.

As can be seen, most of the methods were applied to large-scale civil infrastructure, such as buildings, bridges, and wind turbines, because the advantage of UAV-based vision can be fully exploited. Involving more damage conditions indeed leads to the increasing data acquisition cost.

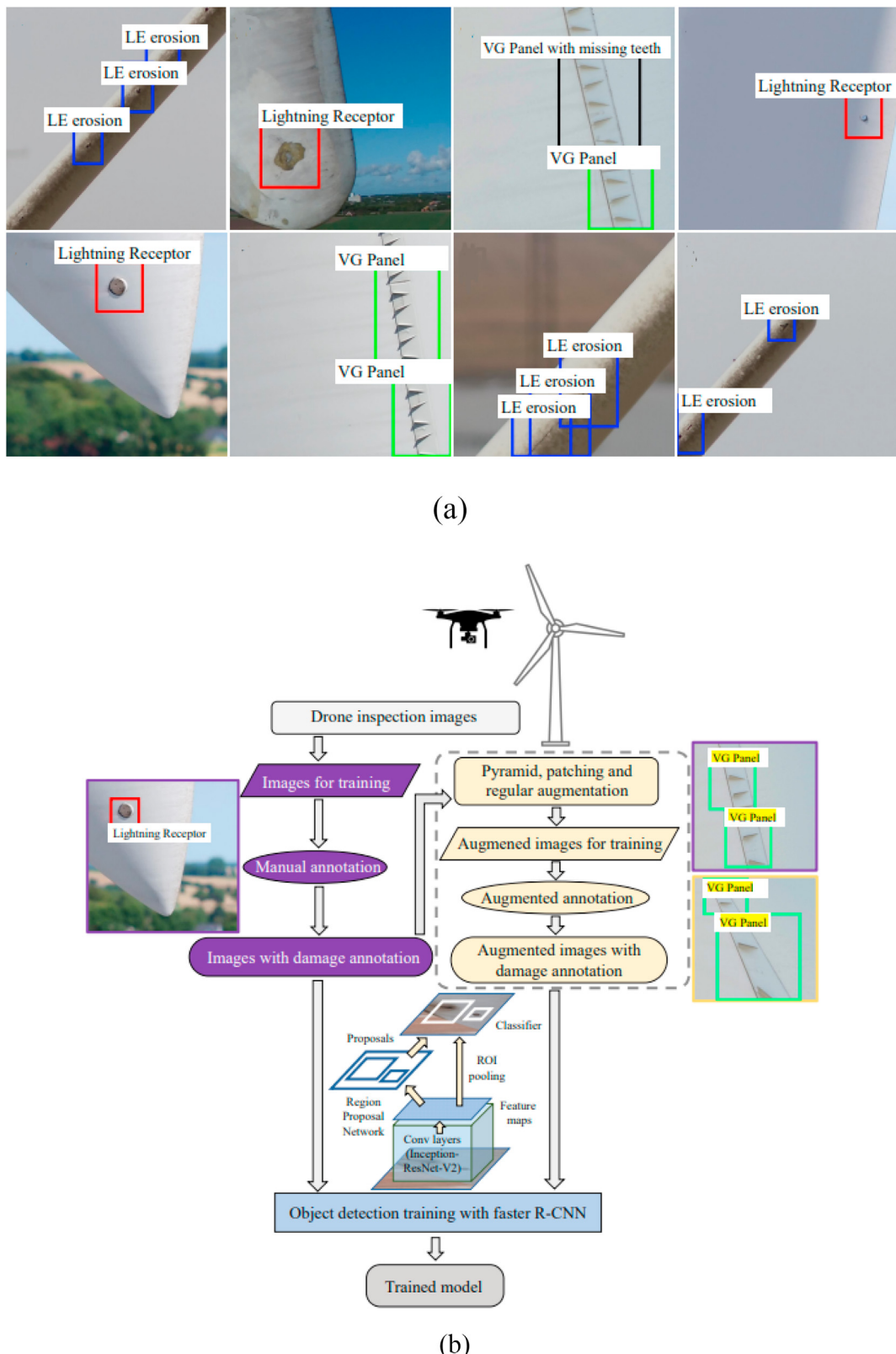


Fig. 5. Wind turbine surface damage detection (a) surface damages/conditions; (b) implementation flowchart (Shihavuddin et al., 2019).

Also, the field image acquisition is conducted on the actual structures, in which the damage progression and occurrence are unpredictable. For these reasons, the damage states considered are limited, and the simple damage detection analysis, i.e., image classification, was mostly carried out.

4.3. Computer vision-based augmented reality and virtual reality

Virtual reality (VR) and augmented reality (AR) are two emerging technologies, offering a new path to gain exciting interactive experiences through computer-generated simulation, which considerably promote

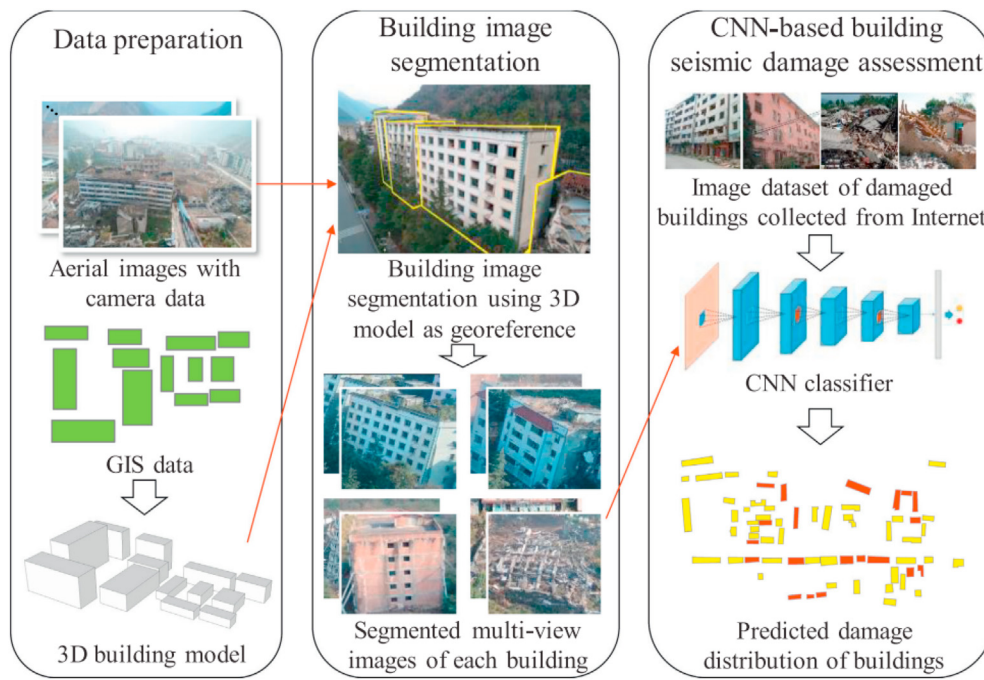


Fig. 6. Framework of the building seismic damage detection. Reprinted with permission from (Xiong et al., 2020).

the research and educational development. VR creates an immersive virtual environment, while AR augments a real-world scene. For damage detection applications, these technologies enable a thorough way of inspecting the target structure and visualizing the possible damage. With the tailored systems equipped, UAV becomes readily capable of creating AR and VR environments by utilizing the controllable flight trajectory. One of the systems is the LiDAR (light detection and ranging) system, which generally consists of a laser, a scanner, and a specialized GPS receiver. The mechanism behind the LiDAR system-equipped UAV is described as 1) sends a light pulse towards the target surface; 2) receives the reflected light to calculate the distance between the UAV and target using the principle, the so-called *Time of Flight* principle (ToF); 3) scans entire target following the designed UAV flight trajectory and create 3-dimensional (3D) point cloud for constructing the interactive environment. It is worth noting that the 3D point cloud can also be directly converted to a physical model to facilitate the inverse model updating-based damage detection. For example, Ghahremani et al. presented a localized approach for updating finite element models based on damage detected in 3D point cloud. This approach can automatically identify and quantify damage by comparing two sets of point clouds of a structural component. The point cloud corresponding to the damage region is then extracted and used to update a solid model of the component, followed by finite element remeshing. This approach avoids the global surface reconstruction and allows for mesh refinement in the localized regions of damage without additional computational cost. Different specimens were used to validate the feasibility of approach (Ghahremani et al., 2018). Castellazzi et al. proposed a semi-automatic method for converting 3D point cloud of a complex object into a 3D finite element model, as shown in Fig. 7. In this method, the point cloud gathered from the terrestrial laser scanner survey is conceived as a stacking of point sections (Fig. 7) (Castellazzi et al., 2015).

While the LiDAR system-equipped UAV is very accurate in surveying, it is expensive and usually is reserved for critical industrial applications. It is noted that the camera-equipped UAV is much cheaper than the LiDAR system-equipped UAV. By fully unleashing the power of computer vision, the camera-equipped UAV can enable VR and AR technologies. One of the prominent computer vision techniques is photogrammetry, also known as photogrammetric computer vision, which adheres to the

same principle of the DIC photogrammetry detailed in Section 3. Noteworthy, some AR and VR development platforms, such as *Unity*, *ARCore*, and *VR Maker by iStaging* with the seamless integration of photogrammetric computer vision have already emerged, which facilitates the creation of VR and AR environments directly from the captured images. Regarding the application of photogrammetric computer vision on UAV-based damage detection, some studies have been found, for example, the virtual reconstruction of a damaged archaeological site using UAV-taken images (Carvajal-Ramírez et al., 2019) (Fig. 8), AR and UAV assisted infrastructure inspection (Note: AR was developed based on *Unity 3D*) (Wen and Kang, 2014), and a UAV and VR-based training and assessment system for bridge inspectors (Note: VR was developed based on *Unity Road Architect*) (Li et al., 2022b).

5. Main challenges and future opportunities for advancement

While UAV enabled computer vision has been increasingly applied to the structural condition assessment over the last several years, the *main challenges* remain open, which are listed as follows.

- Most of the current studies were conducted *offline*. In other words, the UAV-based image acquisition and computer vision enabled damage detection are separate and completed sequentially. Moreover, lab-scale validation or field testing with strictly controlled testing conditions is often carried out. In these cases, the uncertainties that adversely affect damage detection reliability are negligible. Nevertheless, such uncertainties cannot be overlooked in actual practice because the operating conditions of the UAV become unpredictable. Under extreme weather conditions, a large degree of uncertainties may be induced, which makes current UAV configuration and key methodologies inadequate to ensure the desired assessment performance.
- In addition to the abovementioned uncertainties, the dynamic behavior of the target structure is another influential factor to the assessment outcome. For example, the blade rotational speed of the offshore wind turbine may be extremely high and inconstant. Current digital imaging processing methods thus lead to degraded measurement accuracy because of the difficulty in accurately subtracting the

Table 3

Summary of the state-of-the-art deep learning methods/models used for computer vision empowered structural condition assessment.

Reference	Method Description	Analysis Type	Application	Problem Description	Outcome
Yamaguchi et al. (2008)	AlexNet transfer learning	Image classification	Crack detection on concrete surfaces	Two structural conditions, i.e., crack and non-crack conditions (Note: binary classification)	Better detection performance, i.e., both detection accuracy and resolution, than various edge detection methods
Santos et al. (2022)	AlexNet transfer learning; data augmentation		Detection of exposed steel rebars in concretes	Two conditions, i.e., exposed rebar and intact concrete surface (Note: binary classification)	Above 95% for all classification criteria in prediction
Xiong et al. (2020)	VGG-16 transfer learning		Building seismic damage detection	Several damage states of the building; expert judgment for damage states labeling	89.39% prediction accuracy; prediction of the region-based distribution of building damages
GopalakrishnanKasthuriranganGholmi et al. (2018)	VGG-16 transfer learning		Crack detection of common civil infrastructure, such as storage silos, local roadways	Two structural conditions, i.e., crack and non-crack conditions (Note: binary classification)	Up to 90% prediction accuracy in the case study
Choi et al. (2021)	VGG-16 transfer learning with divided sections of image fed to avoid information loss; feature-based image processing		Building crack detection and localization	Two structural conditions, i.e., crack and non-crack conditions (Note: binary classification)	Above 90% prediction accuracy in all formulated cases; the crack location estimation
Samma et al. (2021)	VGG-19 transfer learning with two-layer optimizer		Road damage detection	Two road conditions, i.e., abnormal and normal conditions (Note: binary classification)	96.4% F1-score accuracy in prediction; model training optimizer with enhanced performance
Giefer et al. (2020)	Quantized neural network implemented on a field-programmable gate array (FPGA)		Wind turbine blade surface damage detection	Two structural conditions, i.e., defect and non-defect conditions	Memory access reduction in computation while maintaining desired classification accuracy
Zhang et al. (2022)	Attention-based MobileNetv1-YOLO-v4 with transfer learning; image augmentation		Wind turbine blade defect detection	Two structural conditions, i.e., surface spalling, pitting, crack, and contamination	Improved detection accuracy with significantly faster response speed because of less computational complexity
Xiaoxun et al. (2022)	Multivariate Information (MI)-YOLO model with C3TR module and Alpha-IOU (a loss function)		Wind turbine blade crack detection	Two structural conditions, i.e., defect and non-defect conditions	Improved detection ability of light color cracks under data sample unbalance; the promise of early crack detection
Reddy et al. (2019)	Customized CNN		Detection of cracks and damage in wind turbine blades	Problem 1: two structural conditions, i.e., faulty and non-damage conditions Problem 2: nine different structural conditions	94.5% and 90.6% prediction accuracy for the binary and multiclass classification analysis; a simple index web page with user friendly features for damage detection analysis
Naito et al. (2020)	Customized CNN		Detection of damaged buildings after Kumamoto earthquake	Four different building damage levels considered	81% prediction accuracy, which is much better than support vector machine model; high generalization performance
Pan and Yang (2020)	YOLO-v2		Detection of critical damage states of reinforced concrete buildings	4 damage states in terms of severity levels considered	84.2% Mean Average Precision (MAP) in the prediction that has 7.5% improvement compared to the benchmark methods
Shihavuddin et al. (2019)	Inception-ResNet-V2 architecture-based deep learning; image augmentation	Object detection	Wind turbine blade surface damage detection	Four different surface damages/conditions to be detected/marked from the blade image	81.1% Mean Average Precision (MAP)
Kim et al. (2018)	R-CNN-based transfer learning; planar marker method		Crack identification of an aging concrete bridge	Crack to be detected/ marked from the bridge image (Note: only crack and background in the image)	Desired performance of both crack detection and quantification
Alzarrad et al. (2022)	YOLO-v5		Roof damage detection and condition assessment	Damage to be detected/ marked from the roof image (Note: only damage and background in the image)	81% prediction accuracy

(continued on next page)

Table 3 (continued)

Reference	Method Description	Analysis Type	Application	Problem Description	Outcome
Wu et al. (2019b)	MobileNet with single shot multi-box detector (SSD)		Asphalt pavement condition assessment	12 asphalt pavement distress types to be detected from the road image	Good preliminary result that lays a foundation for autonomous and real-time application
Ayele et al. (2020)	Mask RCNN; Portable network graphics (PNG) masks	Image segmentation (including both semantic and instance segmentations)	Bridge crack detection	Crack to be identified/segmented from the bridge image (Note: only crack and background in the image; pixel binary classification)	Up to 90% prediction accuracy; provides the crack size measurement; a graphic user interface (GUI) for crack detection
Bhowmick et al. (2020)	U-net combined with boundary tracing morphological operation		Detection of cracks on concrete surfaces	Crack to be identified/segmented from the concrete surface image (Note: only crack and background in the image; pixel binary classification)	Desired detection performance of cracks on the concrete surface, quantification of its geometric properties of cracks
Bai et al. (2020b)	Mask R-CNN + HRNet		Damage detection of the structures in extreme events	Damage to be identified/segmented from the structure image (Note: only crack and background in the image; pixel binary classification)	Improved accuracy by testing different earthquake image data as compared to that of benchmark methods

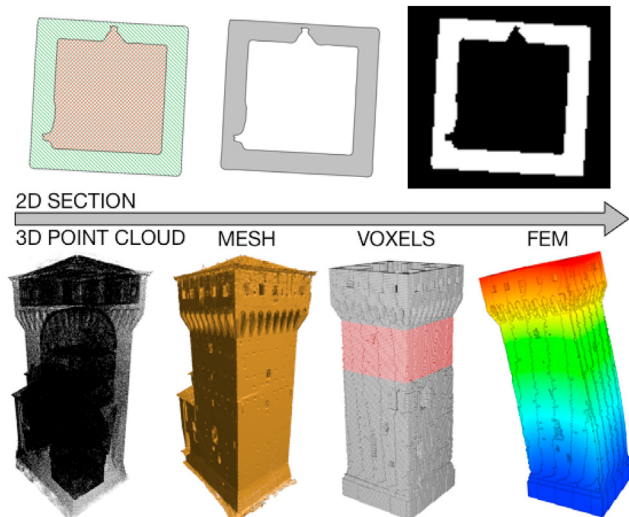


Fig. 7. Conversion from point cloud to 3-D finite element model for masonry tower (Castellazzi et al., 2015).

rigid body motion from the entire motion. Similarly, deep learning-based direct damage detection is limited by the bad image quality caused by fast motion. It is also worth pointing out that while the digital image correlation (DIC) is the most robust image processing method for vibration extraction, the deployment of the artificial speckle patterns, such as the retroreflective markers, usually is labor intensive.

• For damage detection, it is found that all associated studies discussed throughout the manuscript only consider the damage types. However, damage also can be characterized in terms of the severity level (represented by a continuous value). Identifying both the damage types and severity to thoroughly assess the structural condition hence is necessary. Besides, the damage conditions occurred in the in-service structure may be beyond the damage conditions involved in the training dataset. It will become a more common situation, especially when the damage severity is considered. Therefore, deep learning is expected to possess extended inference capacity.

- While significant effort has been made to advance the UAV-based damage detection capacity, an autonomous, robust, real-time UAV-based condition assessment system that serves practical implementations is lacking, which is due to the following difficulties: 1). Data communication and exchange when adopting a wireless UAV network is hardware resource demanding. Data compression and reconstruction can reduce such dependency, which, however, increases the execution time. 2). To deliver reliable damage detection outcomes, sophisticated computer vision algorithms need to be developed. As a result, the algorithm implementation becomes time intensive, not to mention the large-sized image data to be handled. 3). Uncertainties and other realistic factors mentioned above make it challenging to develop an intelligent and unified framework to enable the desired condition assessment robustness and reliability.

Given the above challenges, there are *opportunities for advancement*, which are as follows.

- The uncertainty-induced image quality issue can be mitigated from three aspects: 1). Continuous development and enhancement of image preprocessing to minimize the negative effect of uncertainties to a large extent; 2). Incorporating the new hardware components into the UAV system, for example, adding the vibration and wind-flow energy harvesters to convert the extra energy into electricity. Through such UAV design, the UAV power consumption can be reduced, and meanwhile, the UAV becomes more stable during the flight; 3). The uncertainty-aware machine learning and optimization are capable of elucidating the uncertainty effect (i.e., uncertainty quantification) on decision making, thereby reducing false prediction (Cheng et al., 2022a, 2022b; Zhou and Tang, 2021c; Zhou et al., 2022; Liu et al., 2015).
- To fulfill the extended damage detection, the physical knowledge/constraints should be incorporated into the deep learning to establish the so-called physics-informed deep learning. Fundamentally, the inherent physical correlations among different damage types benefit the inference of unknown damage based upon the currently known damages. Identifying the appropriate way to incorporate physical knowledge is the key to pursuing success. However, this appears to be a widely open solution. Considering the proposed deep learning improvement and new feature integration, it becomes imperative to develop a unified deep learning framework.

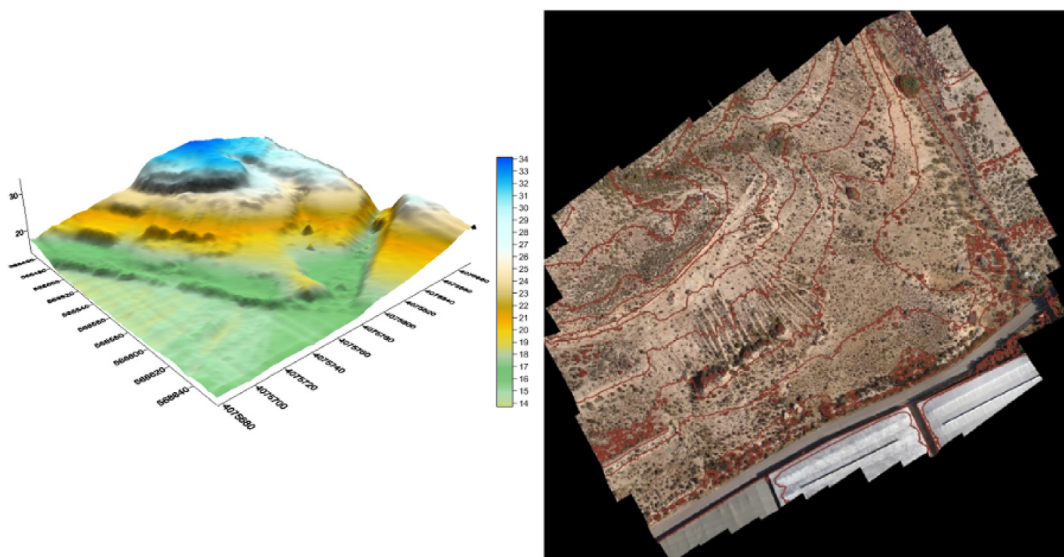


Fig. 8. Digital surface model and orthoimage. Reprinted with permission from (Carvajal-Ramírez et al., 2019).

- Taking advantage of emerging technologies, e.g., the Internet of Things (IoT), cloud computing, and computer vision enabled UAV, one of the future focal points is to establish an autonomous, real-time robust UAV-based condition assessment system. This is an interdisciplinary research requiring the synergistic advancement of the UAV system control, design, and decision-making methodologies and their further seamless integration. The resulting outcome is expected to bridge the gap between the research and applications.

6. Conclusion

In this article, a brief review of utilizing the unmanned aerial vehicle (UAV)-based computer vision for structural vibration measurement and condition assessment is provided. This is a promising and rising research area, in which the high mobility and accessibility of the UAV can be harnessed to advance the capacity and extend the practicability of structural health monitoring and management. The recent development and use of the integral components, i.e., UAV camera system configurations, image processing, and deep learning enabled computer vision, are comprehensively reviewed and discussed from different perspectives. Despite the recent surge, the remaining challenges are also pointed out, along with future directions for potential advancement. Due to the interdisciplinary nature of the research, extensive effort will be made to realize the synergistic advancement of the integral components and then synthesize them seamlessly with emerging technologies, such as the Internet of Things (IoT), cloud computing, collaborative UAVs, etc., for technology evolution.

Declaration of competing interest

The authors declare that they have no known competing financial interests or personal relationships that could have appeared to influence the work reported in this paper.

Acknowledgment

This research is supported by National Science Foundation, United States under grant CMMI-2138522.

References

Abdel-Qader, I., Abudayyeh, O., Kelly, M.E., 2003. Analysis of edge-detection techniques for crack identification in bridges. *J. Comput. Civ. Eng.* 17, 255–263. [https://doi.org/10.1061/\(ASCE\)0887-3801\(2003\)17:4\(255\)](https://doi.org/10.1061/(ASCE)0887-3801(2003)17:4(255)).

Adeagbo, M.O., Lam, H.-F., Ni, Y.Q., 2021. A Bayesian methodology for detection of railway ballast damage using the modified Ludwik nonlinear model. *Eng. Struct.* 236, 112047. <https://doi.org/10.1016/j.engstruct.2021.112047>.

Afolabi, D., Man, K.L., Liang, H.N., Guan, S.U., Krilavicius, T., 2015. Monocular line tracking for the reduction of vibration induced during image acquisition. *J. Vibroengineering.* 17, 655–661.

Ahamed, B.B., Yuvaraj, D., Priya, S.S., 2019. Image denoising with linear and non-linear filters. *Proc. 2019 Int. Conf. Comput. Intell. Knowl. Econ. ICCIKE 2019* 806–810. <https://doi.org/10.1109/ICCIKE47802.2019.9004429>.

Ahmadi, R., Kangarani Farahani, J., Sotudeh, F., Zhaleh, A., Garshasbi, S., 2013. Survey of image denoising techniques. *Life Sci. J.* 10, 753–755. <https://doi.org/10.5120/9288-3488>.

Allouch, A., Koubaa, A., Khalgui, M., Abbes, T., 2019. Qualitative and quantitative risk analysis and safety assessment of unmanned aerial vehicles missions over the internet. *IEEE Access* 7, 53392–53410. <https://doi.org/10.1109/ACCESS.2019.2911980>.

Alzarrad, A., Awolusi, I., Hatamleh, M.T., Terreno, S., 2022. Automatic assessment of roofs conditions using artificial intelligence (AI) and unmanned aerial vehicles (UAVs). *Front. Built Environ.* 8, 1–8. <https://doi.org/10.3389/fbuil.2022.1026225>.

An, J.Y., Il Lee, S., 2022. Phase-based motion magnification for structural vibration monitoring at a video streaming rate. *IEEE Access* 10, 123423–123435. <https://doi.org/10.1109/ACCESS.2022.3224601>.

Andriluka, M., Schnitzspahn, P., Meyer, J., Kohlbrecher, S., Petersen, K., von Stryk, O., Roth, S., Schiele, B., 2010. Vision based victim detection from unmanned aerial vehicles. In: 2010 IEEE/RSJ Int. Conf. Intell. Robot. Syst. IEEE, pp. 1740–1747. <https://doi.org/10.1109/IROS.2010.5649223>.

Avola, D., Cinque, L., Di Mambro, A., Diko, A., et al., 2021. Low-altitude aerial video surveillance via one-class SVM anomaly detection from textural features in UAV images. *Information* 13, 2. <https://doi.org/10.3390/info13010002>.

Ayele, Y.Z., Aliyari, M., Griffiths, D., Drogue, E.L., 2020. Automatic crack segmentation for UAV-assisted bridge inspection. *Energies* 13, 1–16. <https://doi.org/10.3390/en13236250>.

Bai, X., Yang, M., 2021. UAV based accurate displacement monitoring through automatic filtering out its camera's translations and rotations. *J. Build. Eng.* 44, 102992. <https://doi.org/10.1016/j.jobe.2021.102992>.

Bai, X., Yang, M., Ajmera, B., 2020. An advanced edge-detection method for noncontact structural displacement monitoring. *Sensors* 20, 4941. <https://doi.org/10.3390/s20174941>.

Bai, Y., Sezen, H., Yilmaz, A., 2020. End-to-end deep learning methods for automated damage detection in extreme events at various scales. *Proc. - Int. Conf. Pattern Recognit.* 5736–5743. <https://doi.org/10.1109/ICPR48806.2021.9413041>.

Bao, Y., Tang, Z., Li, H., Zhang, Y., 2019. Computer vision and deep learning-based data anomaly detection method for structural health monitoring. *Struct. Health Monit.* 18, 401–421. <https://doi.org/10.1177/1475921718757405>.

Baqersad, J., Poozesh, P., Nizrecks, C., Avitabile, P., 2017. Photogrammetry and optical methods in structural dynamics – a review. *Mech. Syst. Signal Process.* 86, 17–34. <https://doi.org/10.1016/j.ymssp.2016.02.011>.

Bebernick, T.J., Ehrhardt, D.A., 2017. High-speed 3D digital image correlation vibration measurement: recent advancements and noted limitations. *Mech. Syst. Signal Process.* 86, 35–48. <https://doi.org/10.1016/j.ymssp.2016.04.014>.

Bhowmick, S., Nagarajaiah, S., Veeraraghavan, A., 2020. Vision and deep learning-based algorithms to detect and quantify cracks on concrete surfaces from UAV videos. *Sensors* 20, 1–19. <https://doi.org/10.3390/s20216299>.

Bielefeldt, B.R., Hochhalter, J.D., Hartl, D.J., 2018. Shape memory alloy sensory particles for damage detection: experiments, analysis, and design studies. *Struct. Health Monit.* 17, 777–814. <https://doi.org/10.1177/1475921717721194>.

Brunetti, A., Buongiorno, D., Trotta, G.F., Bevilacqua, V., 2018. Computer vision and deep learning techniques for pedestrian detection and tracking: a survey. *Neurocomputing* 300, 17–33. <https://doi.org/10.1016/j.neucom.2018.01.092>.

Cai, C., Meng, H., Zhu, Q., 2018. Blind deconvolution for image deblurring based on edge enhancement and noise suppression. *IEEE Access* 6, 58710–58718. <https://doi.org/10.1109/ACCESS.2018.2874980>.

Caو, P., Zhang, Y., Zhou, K., Tang, J., 2023. A reinforcement learning hyper-heuristic in multi-objective optimization with application to structural damage identification. *Struct. Multidiscip. Optim.* 66, 16. <https://doi.org/10.1007/s00158-022-03432-5>.

Carvaljal-Ramírez, F., Navarro-Ortega, A.D., Agüera-Vega, F., Martínez-Carricundo, P., Mancini, F., 2019. Virtual reconstruction of damaged archaeological sites based on Unmanned Aerial Vehicle Photogrammetry and 3D modelling. Study case of a southeastern Iberia production area in the Bronze Age. *Measurement* 136, 225–236. <https://doi.org/10.1016/j.measurement.2018.12.092>.

Castellazzi, G., D'Altri, A., Bitelli, G., Selvaggi, I., Lambertini, A., 2015. From laser scanning to finite element analysis of complex buildings by using a semi-automatic procedure. *Sensors* 15, 18360–18380. <https://doi.org/10.3390/s150818360>.

Chen, G., Liang, Q., Zhong, W., Gao, X., Cui, F., 2021. Homography-based measurement of bridge vibration using UAV and DIC method. *Measurement* 170, 108683. <https://doi.org/10.1016/j.measurement.2020.108683>.

Chen, J., Liu, D., 2021. Bottom-up image detection of water channel slope damages based on superpixel segmentation and support vector machine. *Adv. Eng. Inf.* 47, 101205. <https://doi.org/10.1016/j.aei.2020.101205>.

Chen, J.G., Wadhwa, N., Cha, Y.-J., Durand, F., Freeman, W.T., Buyukozturk, O., 2015. Modal identification of simple structures with high-speed video using motion magnification. *J. Sound Vib.* 345, 58–71. <https://doi.org/10.1016/j.jsv.2015.01.024>.

Cha, Y.-J., Chen, J.G., Büyüköztürk, O., 2017. Output-only computer vision based damage detection using phase-based optical flow and unscented Kalman filters. *Eng. Struct.* 132, 300–313. <https://doi.org/10.1016/j.engstruct.2016.11.038>.

Chen, J.G., Adams, T.M., Sun, H., Bell, E.S., Büyüköztürk, O., 2018. Camera-based vibration measurement of the world war I memorial bridge in Portsmouth, New Hampshire. *J. Struct. Eng.* 144. [https://doi.org/10.1061/\(ASCE\)ST.1943-541X.0002203](https://doi.org/10.1061/(ASCE)ST.1943-541X.0002203).

Cheng, C., Behzadan, A.H., Noshadrvan, A., 2022. Uncertainty-aware convolutional neural network for explainable artificial intelligence-assisted disaster damage assessment. *Struct. Control Health Monit.* 29. <https://doi.org/10.1002/stc.3019>.

Cheng, C.-S., Behzadan, A.H., Noshadrvan, A., 2022. Bayesian inference for uncertainty-aware post-disaster damage assessment using artificial intelligence. In: *Comput. Civ. Eng.* 2021. American Society of Civil Engineers, Reston, VA, pp. 156–163. <https://doi.org/10.1061/9780784483893.020>.

Choi, S., Kim, E., 2015. Building crack inspection using small UAV. In: 2015 17th Int. Conf. Adv. Commun. Technol. IEEE, pp. 235–238. <https://doi.org/10.1109/ICACT.2015.7224792>.

Choi, D., Bell, W., Kim, D., Kim, J., 2021. UAV-driven structural crack detection and location determination using convolutional neural networks. *Sensors* 21, 1–20. <https://doi.org/10.3390/s21082650>.

Cu, H.X., Wang, Y.Q., Zhang, F.F., Li, T.T., 2018. A motion detection approach based on UAV image sequence. *KSII Trans. Internet Inf. Syst.* 12, 1224–1242. <https://doi.org/10.3837/tii.2018.03.014>.

Davis, A.M., Mirsayar, M., Hartl, D.J., 2021. A novel structural health monitoring approach in concrete structures using embedded magnetic shape memory alloy components. *Construct. Build. Mater.* 311, 125212. <https://doi.org/10.1016/j.conbuildmat.2021.125212>.

Deng, W., Mou, Y., Kashiwa, T., Escalera, S., Nagai, K., Nakayama, K., Matsuo, Y., Prendinger, H., 2020. Vision based pixel-level bridge structural damage detection using a link ASPP network. *Autom. Construc.* 110, 102973. <https://doi.org/10.1016/j.autcon.2019.102973>.

Dhankhar, P., Sahu, N., 2013. A review and research of edge detection techniques for image segmentation related papers A review and research of edge detection techniques for image segmentation. *IJCSCM* J 2, 86–92.

Dong, C.-Z., Catbas, F.N., 2021. A review of computer vision-based structural health monitoring at local and global levels. *Struct. Health Monit.* 20, 692–743. <https://doi.org/10.1177/1475921720935585>.

Ettrier, M., Miller, B., Sirohi, J., Tinney, C., 2021. Effect of broad-band phase-based motion magnification on modal parameter estimation. *Mech. Syst. Signal Process.* 146, 106995. <https://doi.org/10.1016/j.ymssp.2020.106995>.

Ekkachai, K., Leelasawakasut, T., Chaopramualkul, W., Komin, U., Kwansud, P., Bunnun, P., Komeswarakul, P., Tantaworasilp, A., Seekhao, P., Nithi-utthai, S., Pudson, P., Vimolmongkolpon, V., Prakancharoen, S., Chaithan, R., Sothisansern, P., Surinkon, C., Covanch, W., Tungpimolrut, K., 2022. Development of the generator inspection vehicle and the inspection equipment. *J. Field Robot.* 39, 1033–1053. <https://doi.org/10.1002/rob.22086>.

Eschmann, C., Kuo, C.M., Kuo, C.H., Boller, C., 2012. Unmanned aircraft systems for remote building inspection and monitoring. In: *Proc. 6th Eur. Work. - Struct. Heal. Monit.* 2012. EWSHM 2012, pp. 1179–1186.

Esmaeili, F., Ebadi, H., Saadatseresht, M., Kalantary, F., 2019. Application of UAV photogrammetry in displacement measurement of the soil nail walls using local features and CPDA method. *ISPRS Int. J. Geo-Inf.* 8, 25. <https://doi.org/10.3390/ijgi8010025>.

Fan, X., Li, J., Hao, H., Ma, S., 2018. Identification of minor structural damage based on electromechanical impedance sensitivity and sparse regularization. *J. Aero. Eng.* 31. [https://doi.org/10.1061/\(ASCE\)AS.1943-5525.0000892](https://doi.org/10.1061/(ASCE)AS.1943-5525.0000892).

Fan, L., Zhang, F., Fan, H., Zhang, C., 2019. Brief review of image denoising techniques. *Vis. Comput. Ind. Biomed. Art.* 2, 7. <https://doi.org/10.1186/s42492-019-0016-7>.

Feng, D., Feng, M.Q., 2018. Computer vision for SHM of civil infrastructure: from dynamic response measurement to damage detection – a review. *Eng. Struct.* 156, 105–117. <https://doi.org/10.1016/j.engstruct.2017.11.018>.

Ferrer, B., Acevedo, P., Espinosa, J., Mas, D., 2015. Targetless image-based method for measuring displacements and strains on concrete surfaces with a consumer camera. *Construct. Build. Mater.* 75, 213–219. <https://doi.org/10.1016/j.conbuildmat.2014.11.019>.

Galantucci, R.A., Fatiguso, F., 2019. Advanced damage detection techniques in historical buildings using digital photogrammetry and 3D surface analysis. *J. Cult. Herit.* 36, 51–62. <https://doi.org/10.1016/j.jculher.2018.09.014>.

Genceturk, B., Hossain, K., Kapadia, A., Labib, E., Mo, Y.-L., 2014. Use of digital image correlation technique in full-scale testing of prestressed concrete structures. *Measurement* 47, 505–515. <https://doi.org/10.1016/j.measurement.2013.09.018>.

Ghahremani, K., Khaloo, A., Mohamadi, S., Lattanzi, D., 2018. Damage detection and finite-element model updating of structural components through point cloud analysis. *J. Aero. Eng.* 31. [https://doi.org/10.1061/\(ASCE\)AS.1943-5525.0000885](https://doi.org/10.1061/(ASCE)AS.1943-5525.0000885).

Giefer, L.A., Staar, B., Freitag, M., 2020. FPGA-based optical surface inspection of wind turbine rotor blades using quantized neural networks. *Electronics* 9, 1824. <https://doi.org/10.3390/electronics9111824>.

Gopalakrishnan, A., Kasthurirangan, Gholmi, Hoda, Vidyadharan, Akash, Choudhary, Alok, Agrawal, 2018. Crack damage detection in unmanned aerial vehicle images of civil infrastructure using pre-trained deep learning model. *Int. J. Traffic Transport. Eng.* 8, 1–14. [https://doi.org/10.7708/ijtte.2018.8\(1\).01](https://doi.org/10.7708/ijtte.2018.8(1).01).

Hallermann, N., Morgenstern, G., 2014. Visual inspection strategies for large bridges using unmanned aerial vehicles (UAV), bridge Maintenance, safety, manag. Life Ext. - Proc. 7th Int. Conf. Bridg. Maintenance, Saf. Manag. IABMAS 2014 661–667. <https://doi.org/10.1201/b17063-96>.

Han, Y., Wu, G., Feng, D., 2022. Vision-based displacement measurement using an unmanned aerial vehicle. *Struct. Control Health Monit.* 29. <https://doi.org/10.1002/stc.3025>.

Havaran, A., Mahmoudi, M., 2020. Extracting structural dynamic properties utilizing close photogrammetry method. *Measurement* 150, 107092. <https://doi.org/10.1016/j.measurement.2019.107092>.

Helfrick, M.N., Niegrecki, C., Avitabile, P., Schmidt, T., 2011. 3D digital image correlation methods for full-field vibration measurement. *Mech. Syst. Signal Process.* 25, 917–927. <https://doi.org/10.1016/j.ymssp.2010.08.013>.

Hisham, M.B., Yaakob, S.N., Raof, R.A., Nazren, A.A., Wafi, N.M., 2015. Template matching using sum of squared difference and normalized cross correlation. In: 2015 IEEE Student Conf. Res. Dev. IEEE, pp. 100–104. <https://doi.org/10.1109/SCORED.2015.7449303>.

Hou, R., Xia, Y., Zhou, X., 2018. Structural damage detection based on l1 regularization using natural frequencies and mode shapes. *Struct. Control Health Monit.* 25, e2107. <https://doi.org/10.1002/stc.2107>.

Hua, X.G., Ni, Y.Q., Chen, Z.Q., Ko, J.M., 2008. An improved perturbation method for stochastic finite element model updating. *Int. J. Numer. Methods Eng.* 73, 1845–1864. <https://doi.org/10.1002/nme.2151>.

Huang, X., Liu, Z., Zhang, X., Kang, J., Zhang, M., Guo, Y., 2020. Surface damage detection for steel wire ropes using deep learning and computer vision techniques. *Measurement* 161, 107843. <https://doi.org/10.1016/j.measurement.2020.107843>.

Huňády, R., Pavelka, P., Lengvárský, P., 2019. Vibration and modal analysis of a rotating disc using high-speed 3D digital image correlation. *Mech. Syst. Signal Process.* 121, 201–214. <https://doi.org/10.1016/j.ymssp.2018.11.024>.

Ichi, E., Dorafshan, S., 2022. Effectiveness of infrared thermography for delamination detection in reinforced concrete bridge decks. *Autom. Construc.* 142, 104523. <https://doi.org/10.1016/j.autcon.2022.104523>.

Jang, K., An, Y., Kim, B., Cho, S., 2021. Automated crack evaluation of a high-rise bridge pier using a ring-type climbing robot. *Comput. Civ. Infrastruct. Eng.* 36, 14–29. <https://doi.org/10.1111/mice.12550>.

Javed, A., Lee, H., Kim, B., Han, Y., 2022. Vibration measurement of a rotating cylindrical structure using subpixel-based edge detection and edge tracking. *Mech. Syst. Signal Process.* 166, 104837. <https://doi.org/10.1016/j.ymssp.2021.104837>.

Kakooei, M., Baleghi, Y., 2017. Fusion of satellite, aircraft, and UAV data for automatic disaster damage assessment. *Int. J. Rem. Sens.* 38, 2511–2534. <https://doi.org/10.1080/01431161.2017.1294780>.

Kerwin, W., 2009. Image processing and analysis in tagged cardiac MRI. In: *Handb. Med. Image Process. Anal.* Elsevier, pp. 435–452. <https://doi.org/10.1016/B978-012373904-9.50035-0>.

Khadka, A., Fick, B., Afshar, A., Tavakoli, M., Baqersad, J., 2020. Non-contact vibration monitoring of rotating wind turbines using a semi-autonomous UAV. *Mech. Syst. Signal Process.* 138, 106446. <https://doi.org/10.1016/j.ymssp.2019.106446>.

Khadka, A., Afshar, A., Zadeh, M., Baqersad, J., 2022. Strain monitoring of wind turbines using a semi-autonomous drone. *Wind Eng.* 46, 296–307. <https://doi.org/10.1177/0309524X211027814>.

Khan, N.A., Jhanjhi, N.Z., Brohi, S.N., Usmani, R.S.A., Nayyar, A., 2020. Smart traffic monitoring system using unmanned aerial vehicles (UAVs), comput. Commun. Now. 157, 434–443. <https://doi.org/10.1016/j.comcom.2020.04.049>.

Khuc, T., Nguyen, T.A., Dao, H., Catbas, F.N., 2020. Swaying displacement measurement for structural monitoring using computer vision and an unmanned aerial vehicle. *Measurement* 159, 107769. <https://doi.org/10.1016/j.measurement.2020.107769>.

Kim, H., Lee, J., Ahn, E., Cho, S., Shin, M., Sim, S.-H., 2017. Concrete crack identification using a UAV incorporating hybrid image processing. *Sensors* 17, 2052. <https://doi.org/10.3390/s17092052>.

Kim, I.H., Jeon, H., Baek, S.C., Hong, W.H., Jung, H.J., 2018. Application of crack identification techniques for an aging concrete bridge inspection using an unmanned aerial vehicle. In: *Sensors*, pp. 1–14. <https://doi.org/10.3390/s18061881> (Switzerland).

Kudela, P., Wandowski, T., Malinowski, P., Ostachowicz, W., 2017. Application of scanning laser Doppler vibrometry for delamination detection in composite

structures. *Opt Laser. Eng.* 99, 46–57. <https://doi.org/10.1016/j.optlaseng.2016.10.022>.

Kumarapu, K., Mesapam, S., Keesara, V.R., Shukla, A.K., Manapragada, N.V.S.K., Javed, B., 2022. RCC structural deformation and damage quantification using unmanned aerial vehicle image correlation technique. *Appl. Sci.* 12, 6574. <https://doi.org/10.3390/app12136574>.

La, A., Salmon, J., Ellingson, J., 2019. Development of a Semi-autonomous Drone for Structural Health Monitoring of Structures Using Digital Image Correlation (DIC). <https://gen.lib.rus.ec/book/index.php?md5=99bab0160d648466085b4eb95039f7ed>.

Lee, A.J., Song, W., Yu, B., Choi, D., Tirtawardhana, C., Myung, H., 2023. Survey of robotics technologies for civil infrastructure inspection. *J. Infrastruct. Intell. Resil.* 2, 100018. <https://doi.org/10.1016/j.intel.2022.100018>.

Lei, B., Wang, N., Xu, P., Song, G., 2018. New crack detection method for bridge inspection using UAV incorporating image processing. *J. Aero. Eng.* 31. [https://doi.org/10.1061/\(ASCE\)AS1943-5525.0000879](https://doi.org/10.1061/(ASCE)AS1943-5525.0000879).

Li, W., Zhao, W., Gu, J., Fan, B., Du, Y., 2022. Dynamic characteristics monitoring of large wind turbine blades based on target-free DSST vision algorithm and UAV. *Rem. Sens.* 14, 3113. <https://doi.org/10.3390/rs14133113>.

Li, X., Gao, C., Guo, Y., He, F., Shao, Y., 2019. Cable surface damage detection in cable-stayed bridges using optical techniques and image mosaicking. *Opt Laser. Technol.* 110, 36–43. <https://doi.org/10.1016/j.optlastec.2018.07.012>.

Li, Y., Karim, M.M., Qin, R., 2022. A virtual-reality-based training and assessment system for bridge inspectors with an assistant drone. *IEEE Trans. Human-Machine Syst.* 52, 591–601. <https://doi.org/10.1109/THMS.2022.3155373>.

Liu, G., He, C., Zou, C., Wang, A., 2022. Displacement measurement based on UAV images using SURF-enhanced camera calibration algorithm. *Rem. Sens.* 14, 6008. <https://doi.org/10.3390/rs14236008>.

Liu, Y., Zhou, K., Lei, Y., 2015. Using Bayesian inference framework towards identifying gas species and concentration from high temperature resistive sensor array data. *J. Sens.* 2015, 1–10. <https://doi.org/10.1155/2015/351940>.

Lianpo, W., 2022. Super-robust digital image correlation based on learning template. *Opt. Laser. Eng.* 158, 107164. <https://doi.org/10.1016/j.optlaseng.2022.107164>.

Lu, J., Fang, P., Tian, Y., 2011. An objects detection framework in UAV videos. *Adv. Comput. Sci. Educ. Appl.* 113–119. https://doi.org/10.1007/978-3-642-22456-0_17.

Maio, L., Ricci, F., Memmolo, V., Monaco, E., Boffa, N.D., 2018. Application of laser Doppler vibrometry for ultrasonic velocity assessment in a composite panel with defect. *Compos. Struct.* 184, 1030–1039. <https://doi.org/10.1016/j.comstruct.2017.10.059>.

Mitra, K., Cossairt, O., Veeraghavan, A., 2014. To denoise or deblur: parameter optimization for imaging systems. *Digit. Photo X.* 9023, 90230G. <https://doi.org/10.1117/12.2038819>.

Nagaya, K., Yoshino, T., Katayama, M., Murakami, I., Ando, Y., 2012. Wireless piping inspection vehicle using magnetic adsorption force. *IEEE/ASME Trans. Mechatronics.* 17, 472–479. <https://doi.org/10.1109/TMECH.2011.2182201>.

Naito, S., Tomozawa, H., Mori, Y., Nagata, T., Monma, N., Nakamura, H., Fujiwara, H., Shoji, G., 2020. Building-damage detection method based on machine learning utilizing aerial photographs of the Kumamoto earthquake. *Earthq. Spectra* 36, 1166–1187. <https://doi.org/10.1177/8755293019901309>.

Nakamura, S., Yamashita, A., Inoue, F., Inoue, D., Takahashi, Y., Kamimura, N., Ueno, T., 2019. Inspection test of a tunnel with an inspection vehicle for tunnel lining concrete. *J. Robot. Mechatron.* 31, 762–771. <https://doi.org/10.20965/jrm.2019.p0762>.

Nappo, N., Mavrouli, O., Van Westen, C., Gambillara, R., 2020. Semi-automatic Road Damage Detection in Landslide Areas Using UAV-Based 3D Models, p. 5910. <https://doi.org/10.5194/egusphere-egu2020-5910>.

Nguyen, S.T., La, H.M., 2019. Development of a steel bridge climbing robot. In: 2019 IEEE/RSJ Int. Conf. Intell. Robot. Syst. IEEE, pp. 1912–1917. <https://doi.org/10.1109/IROS40897.2019.8967748>.

Nguyen, S.T., La, H.M., 2021. A climbing robot for steel bridge inspection. *J. Intell. Rob. Syst.* 102, 75. <https://doi.org/10.1007/s10846-020-01266-1>.

Niezrecki, C., Avitabile, P., Warren, C., Pingle, P., Helfrick, M., Tomasini, E.P., 2010. A review of digital image correlation applied to structure dynamics, 219–232. <https://doi.org/10.1063/1.3455461>.

Oliveira, H.C., Guizilini, V.C., Nunes, I.P., Souza, J.R., 2018. Failure detection in row crops from UAV images using morphological operators. *Geosci. Rem. Sens. Lett. IEEE* 15, 991–995. <https://doi.org/10.1109/LGRS.2018.2819944>.

Outay, F., Mengash, H.A., Adnan, M., 2020. Applications of unmanned aerial vehicle (UAV) in road safety, traffic and highway infrastructure management: recent advances and challenges. *Transport. Res. Part A Policy Pract.* 141, 116–129. <https://doi.org/10.1016/j.tra.2020.09.018>.

Ozbek, M., Rixen, D.J., Erne, O., Sanow, G., 2010. Feasibility of monitoring large wind turbines using photogrammetry. *Energy* 35, 4802–4811. <https://doi.org/10.1016/j.energy.2010.09.008>.

Peng, C., Zeng, C., Wang, Y., 2020. Camera-based micro-vibration measurement for lightweight structure using an improved phase-based motion extraction. *IEEE Sensor. J.* 20, 2590–2599. <https://doi.org/10.1109/JSEN.2019.2951128>.

Pan, B., Xie, H., Yang, L., Wang, Z., 2009. Accurate measurement of satellite antenna surface using 3D digital image correlation technique. *Strain* 45, 194–200. <https://doi.org/10.1111/j.1475-1305.2008.00450.x>.

Pan, X., Yang, T.Y., 2020. Postdisaster image-based damage detection and repair cost estimation of reinforced concrete buildings using dual convolutional neural networks. *Comput. Civ. Infrastruct. Eng.* 35, 495–510. <https://doi.org/10.1111/mice.12549>.

Peng, J., Lin, Liu, 2021. Detection and Analysis of Large-scale WT Blade Surface Cracks Based on UAV-taken Images. *IET Image Process.*

Perry, B.J., Guo, Y., 2021. A portable three-component displacement measurement technique using an unmanned aerial vehicle (UAV) and computer vision: a proof of concept. *Measurement* 176, 109222. <https://doi.org/10.1016/j.measurement.2021.109222>.

Pieczonka, Ł., Ambroziński, Ł., Staszewski, W.J., Barnoncel, D., Pérès, P., 2017. Damage detection in composite panels based on mode-converted Lamb waves sensed using 3D laser scanning vibrometer. *Opt. Laser. Eng.* 99, 80–87. <https://doi.org/10.1016/j.optlaseng.2016.12.017>.

Pierce, S.G., Burnham, K.C., Zhang, D., McDonald, L., MacLeod, C.N., Dobie, G., Summan, R., McMahon, D., 2018. Quantitative inspection of wind turbine blades using UAV deployed photogrammetry. In: 9th Eur. Work. Struct. Heal. Monit. EWSHM 2018, pp. 1–12.

Poozesh, P., Sarrafi, A., Mao, Z., Avitabile, P., Niezrecki, C., 2017. Feasibility of extracting operating shapes using phase-based motion magnification technique and stereo-photogrammetry. *J. Sound Vib.* 407, 350–366. <https://doi.org/10.1016/j.jsv.2017.06.003>.

Qiao, P., Lu, K., Lestari, W., Wang, J., 2007. Curvature mode shape-based damage detection in composite laminated plates. *Compos. Struct.* 80, 409–428. <https://doi.org/10.1016/j.compositstruct.2006.05.026>.

Rao, Y., Xiang, B.J., Huang, B., Mao, S., 2019. Wind turbine blade inspection based on unmanned aerial vehicle(UAV) visual systems. In: 2019 IEEE 3rd Conf. Energy Internet Energy Syst. Integr. IEEE, pp. 708–713. <https://doi.org/10.1109/EI247390.2019.9062226>.

Reagan, D., Sabato, A., Niezrecki, C., 2017. Unmanned aerial vehicle acquisition of three-dimensional digital image correlation measurements for structural health monitoring of bridges. *Nondestruct. Charact. Monit. Adv. Mater. Aerospace, Civ. Infrastruct.* 2017, 1016909. <https://doi.org/10.1117/12.2259985>.

Reagan, D., Sabato, A., Niezrecki, C., 2018. Feasibility of using digital image correlation for unmanned aerial vehicle structural health monitoring of bridges. *Struct. Health Monit.* 17, 1056–1072. <https://doi.org/10.1177/1475921717735326>.

Reddy, A., Indragandhi, V., Ravi, L., Subramanyaswamy, V., 2019. Detection of cracks and damage in wind turbine blades using artificial intelligence-based image analytics. *Measurement* 147, 106823. <https://doi.org/10.1016/j.measurement.2019.07.051>.

Report, Q.P., Bas, E., 2022. Towards Autonomous Drone-Based Dynamic and Seismic Response Monitoring of Bridges.

Reu, P.L., Rohe, D.P., Jacobs, L.D., 2017. Comparison of DIC and LDV for practical vibration and modal measurements. *Mech. Syst. Signal Process.* 86, 2–16. <https://doi.org/10.1016/j.ymssp.2016.02.006>.

Ribeiro, D., Santos, R., Cabral, R., Saramago, G., Montenegro, P., Carvalho, H., Correia, J., Calçada, R., 2021. Non-contact structural displacement measurement using Unmanned Aerial Vehicles and video-based systems. *Mech. Syst. Signal Process.* 160, 107869. <https://doi.org/10.1016/j.ymssp.2021.107869>.

Samma, H., Stundi, S.A., Ismail, N.A., Sulaiman, S., Ping, L.L., 2021. Evolving pre-trained CNN using two-layers optimizer for road damage detection from drone images. *IEEE Access* 9, 158215–158226. <https://doi.org/10.1109/ACCESS.2021.3131231>.

Santos, R., Ribeiro, D., Lopes, P., Cabral, R., Calçada, R., 2022. Detection of exposed steel rebars based on deep-learning techniques and unmanned aerial vehicles. *Autom. ConStruct.* 139, 104324. <https://doi.org/10.1016/j.autcon.2022.104324>.

Sanz, J.O., Docampo, M. de la L.G., Rodriguez, S.M., Sanmartín, M.T.R., Cameselle, G.M., 2010. A simple methodology for recording petroglyphs using low-cost digital image correlation photogrammetry and consumer-grade digital cameras. *J. Archaeol. Sci.* 37, 3158–3169. <https://doi.org/10.1016/j.jas.2010.07.017>.

Sarrafi, A., Mao, Z., Niezrecki, C., Poozesh, P., 2018. Vibration-based damage detection in wind turbine blades using Phase-based Motion Estimation and motion magnification. *J. Sound Vib.* 421, 300–318. <https://doi.org/10.1016/j.jsv.2018.01.050>.

Shao, Y., Li, L., Li, J., An, S., Hao, H., 2022. Target-free 3D tiny structural vibration measurement based on deep learning and motion magnification. *J. Sound Vib.* 538, 117244. <https://doi.org/10.1016/j.jsv.2022.117244>.

Shi, Z.Y., Law, S.S., Zhang, L.M., 1998. Structural damage localization from modal strain change. *J. Sound Vib.* 218, 825–844. <https://doi.org/10.1006/jsvi.1998.1878>.

Shihavuddin, A.S.M., Chen, X., Fedorov, V., Christensen, A.N., Riis, N.A.B., Branner, K., Dahl, A.B., Paulsen, R.R., 2019. Wind turbine surface damage detection by deep learning aided drone inspection analysis. *Energies* 12, 1–15. <https://doi.org/10.3390/en12040676>.

Shorten, C., Khoshgoftaar, T.M., 2019. A survey on image data augmentation for deep learning. *J. Big Data* 6, 60. <https://doi.org/10.1186/s40537-019-0197-0>.

Shuai, Q., Zhou, K., Zhou, S., Tang, J., 2017. Fault identification using piezoelectric impedance measurement and model-based intelligent inference with pre-screening. *Smart Mater. Struct.* 26, 045007. <https://doi.org/10.1088/1361-665X/aa5d41>.

Stanbridge, A.B., Ewins, D.J., 1999. Modal testing using a scanning laser Doppler vibrometer. *Mech. Syst. Signal Process.* 13, 255–270. <https://doi.org/10.1006/mssp.1998.1209>.

Sui, H., Tu, J., Song, Z., Chen, G., Li, Q., 2014. A novel 3D building damage detection method using multiple overlapping UAV images. *Int. Arch. Photogramm. Remote Sens. Spat. Inf. Sci. - ISPRS Arch.* 40, 173–179. <https://doi.org/10.5194/isprarchives-XL-7-173-2014>.

Sun, J., Peng, B., Wang, C.C., Chen, K., Zhong, B., Wu, J., 2022. Building displacement measurement and analysis based on UAV images. *Autom. ConStruct.* 140, 104367. <https://doi.org/10.1016/j.autcon.2022.104367>.

Tai, Yu-Wing, Du, Hao, Brown, M.S., Lin, S., 2008. Image/video deblurring using a hybrid camera. In: 2008 IEEE Conf. Comput. Vis. Pattern Recognit. IEEE, pp. 1–8. <https://doi.org/10.1109/CVPR.2008.4587507>.

Taj, G., Anand, S., Haneefi, A., Kanishka, R.P., Mythra, D.H.A., 2020. Monitoring of historical structures using drones. *IOP Conf. Ser. Mater. Sci. Eng.* <https://doi.org/10.1088/1757-899X/955/1/012008>, 0–6.

Thompson, L.J., Puntel, L.A., 2020. Transforming unmanned aerial vehicle (UAV) and multispectral sensor into a practical decision support system for precision nitrogen management in corn. *Rem. Sens.* 12, 1597. <https://doi.org/10.3390/rs12101597>.

Trebuña, F., Hagara, M., 2014. Experimental modal analysis performed by high-speed digital image correlation system. *Measurement* 50, 78–85. <https://doi.org/10.1016/j.measurement.2013.12.038>.

Ullah, F., Kaneko, S., 2004. Using orientation codes for rotation-invariant template matching. *Pattern Recogn.* 37, 201–209. [https://doi.org/10.1016/S0031-3203\(03\)00184-5](https://doi.org/10.1016/S0031-3203(03)00184-5).

Wadhwa, N., Rubinstein, M., Durand, F., Freeman, W.T., 2013. Phase-based video motion processing. *ACM Trans. Graph.* 32, 1–10. <https://doi.org/10.1145/2461912.2461966>.

Wang, R., Tao, D., 2014. Recent Progress in Image Deblurring. <http://arxiv.org/abs/1409.6838>.

Wang, D., Song, H., Zhu, H., 2013. Numerical and experimental studies on damage detection of a concrete beam based on PZT admittances and correlation coefficient. *Construct. Build. Mater.* 49, 564–574. <https://doi.org/10.1016/j.conbuildmat.2013.08.074>.

Wang, Z., Zhang, K., Chen, Y., Luo, Z., Zheng, J., 2017. A real-time weld line detection for derusting wall-climbing robot using dual cameras. *J. Manuf. Process.* 27, 76–86. <https://doi.org/10.1016/j.jmapro.2017.04.002>.

Wang, J., Liu, X.-Z., Ni, Y.-Q., 2018. A bayesian probabilistic approach for acoustic emission-based rail condition assessment. *Comput. Civ. Infrastruct. Eng.* 33, 21–34. <https://doi.org/10.1111/mice.12316>.

Wang, W., Li, X., Ahmat, Y., Hu, X., Chen, A., 2019. Vibration measurement method based on point tracking for irregular structures. *Optik* 176, 482–490. <https://doi.org/10.1016/j.ijleo.2018.09.100>.

Wang, S., Rodgers, C., Zhai, G., Matiki, T.N., Welsh, B., Najafi, A., Wang, J., Narazaki, Y., Hoskere, V., Spencer, B.F., 2022. A graphics-based digital twin framework for computer vision-based post-earthquake structural inspection and evaluation using unmanned aerial vehicles. *J. Infrastruct. Intell. Resil.* 1, 100003. <https://doi.org/10.1016/j.jiintell.2022.100003>.

Wang, L., Yang, J., Huang, C., Luo, X., 2022. An improved U-Net model for segmenting wind turbines from UAV-taken images. *IEEE Sensors Lett* 6, 1–4. <https://doi.org/10.1109/LSENS.2022.3184521>.

Wen, M.C., Kang, S.C., 2014. Augmented reality and unmanned aerial vehicle assist in construction management. In: *Comput. Civ. Build. Eng. - Proc. 2014 Int. Conf. Comput. Civ. Build. Eng.*, pp. 1570–1577. <https://doi.org/10.1061/9780784413616.195>.

Weng, S., Xia, Y., Xu, Y.-L., Zhu, H.-P., 2011. Substructure based approach to finite element model updating. *Comput. Struct.* 89, 772–782. <https://doi.org/10.1016/j.compstruc.2011.02.004>.

Weng, Y., Shan, J., Lu, Z., Lu, X., Spencer, B.F., 2021. Homography-based structural displacement measurement for large structures using unmanned aerial vehicles. *Comput. Civ. Infrastruct. Eng.* 36, 1114–1128. <https://doi.org/10.1111/mice.12645>.

Wipf, D., Zhang, H., 2015. Revisiting Bayesian blind deconvolution. *J. Mach. Learn. Res.* 15, 3595–3634.

Wu, Z.Y., Zhou, K., Shenton, H.W., Chajes, M.J., 2019. Development of sensor placement optimization tool and application to large-span cable-stayed bridge. *J. Civ. Struct. Heal. Monit.* 9, 77–90. <https://doi.org/10.1007/s13349-018-0320-5>.

Wu, W., Qurishee, M.A., Owino, J., Fomunung, I., Onyango, M., Atolagbe, B., 2019. Coupling deep learning and UAV for infrastructure condition assessment automation. 2018 IEEE Int. Smart Cities Conf. ISCC 2018. <https://doi.org/10.1109/ISC2.2018.8656971>.

Wu, H., Nie, G., Fan, X., 2020. Comparison of buildings extraction algorithms based on small UAV aerial images. In: Di Martino, S., Fang, Z., Li, K.-J. (Eds.), *Web Wirel. Geogr. Inf. Syst.* Springer International Publishing, Cham, pp. 95–101.

Wu, Z., Chen, G., Ding, Q., Yuan, B., Yang, X., 2021. Three-dimensional reconstruction-based vibration measurement of bridge model using UAVs. *Appl. Sci.* 11, 5111. <https://doi.org/10.3390/app11115111>.

Xia, Y., Hao, H., Brownjohn, J.M.W., Xia, P.-Q., 2002. Damage identification of structures with uncertain frequency and mode shape data. *Earthq. Eng. Struct. Dynam.* 31, 1053–1066. <https://doi.org/10.1002/eqe.137>.

Xiaoxun, Z., Xinyu, H., Xiaoxia, G., Xing, Y., Zixu, X., Yu, W., Huixin, L., 2022. Research on crack detection method of wind turbine blade based on a deep learning method. *Appl. Energy* 328, 120241. <https://doi.org/10.1016/j.apenergy.2022.120241>.

Xiong, C., Li, Q., Lu, X., 2020. Automated regional seismic damage assessment of buildings using an unmanned aerial vehicle and a convolutional neural network. *Autom. ConStruct.* 109, 102994. <https://doi.org/10.1016/j.autcon.2019.102994>.

Xu, Y., Brownjohn, J.M.W., 2018. Review of machine-vision based methodologies for displacement measurement in civil structures. *J. Civ. Struct. Heal. Monit.* 8, 91–110. <https://doi.org/10.1007/s13349-017-0261-4>.

Yamaguchi, T., Nakamura, S., Saegusa, R., Hashimoto, S., 2008. Image-based crack detection for real concrete surfaces. *IEEJ Trans. Electr. Electron. Eng.* 3, 128–135. <https://doi.org/10.1002/tee.20244>.

Yan, G., Li, L., Coy, A., Mu, X., Chen, S., Xie, D., Zhang, W., Shen, Q., Zhou, H., 2019. Improving the estimation of fractional vegetation cover from UAV RGB imagery by colour unmixing. *ISPRS J. Photogrammetry Remote Sens.* 158, 23–34. <https://doi.org/10.1016/j.isprsjprs.2019.09.017>.

Yan, Z., Jin, Z., Teng, S., Chen, G., Bassir, D., 2022. Measurement of bridge vibration by UAVs combined with CNN and KLT optical-flow method. *Appl. Sci.* 12, 5181. <https://doi.org/10.3390/app12105181>.

Yang, Y., Dorn, C., Mancini, T., Talken, Z., Kenyon, G., Farrar, C., Mascareñas, D., 2017. Blind identification of full-field vibration modes from video measurements with phase-based video motion magnification. *Mech. Syst. Signal Process.* 85, 567–590. <https://doi.org/10.1016/j.jymssp.2016.08.041>.

Ye, X., Jin, T., Ang, P., Bian, X., Chen, Y., 2021. Computer vision-based monitoring of the 3-D structural deformation of an ancient structure induced by shield tunneling construction. *Struct. Control Health Monit.* 28. <https://doi.org/10.1002/stc.2702>.

Yu, H., Yang, W., Zhang, H., He, W., 2017. A UAV-based crack inspection system for concrete bridge monitoring. In: 2017 IEEE Int. Geosci. Remote Sens. Symp. IEEE, pp. 3305–3308. <https://doi.org/10.1109/IGARSS.2017.8127704>.

Yuan, C., Xiong, B., Li, X., Sang, X., Kong, Q., 2022. A novel intelligent inspection robot with deep stereo vision for three-dimensional concrete damage detection and quantification. *Struct. Health Monit.* 21, 788–802. <https://doi.org/10.1177/14759217211010238>.

Zacharie, M., Fuji, S., Minori, S., 2018. Rapid human body detection in disaster sites using image processing from unmanned aerial vehicle (UAV) cameras. In: 2018 Int. Conf. Intell. Informatics Biomed. Sci. IEEE, pp. 230–235. <https://doi.org/10.1109/ICIIBMS.2018.8549955>.

Zhang, D., Burnham, K., McDonald, L., MacLeod, C., Dobie, G., Summan, R., Pierce, G., 2017. Remote inspection of wind turbine blades using UAV with photogrammetry payload. In: 56th Annu. Conf. Br. Inst. Non-destructive Testing. NDT 2017, pp. 1–11.

Zhang, C., Chang, C., Jamshidi, M., 2020. Concrete bridge surface damage detection using a single-stage detector. *Comput. Civ. Infrastruct. Eng.* 35, 389–409. <https://doi.org/10.1111/mice.12500>.

Zhang, F., Hu, Z., Fu, Y., Yang, K., Wu, Q., Feng, Z., 2020. A new identification method for surface cracks from UAV images based on machine learning in coal mining areas. *Rem. Sens.* 12, 1571. <https://doi.org/10.3390/rs12101571>.

Zhang, J., Wu, Z., Chen, G., Liang, Q., 2021. Comparisons of differential filtering and homography transformation in modal parameter identification from UAV measurement. *Sensors* 21, 5664. <https://doi.org/10.3390/s21165664>.

Zhang, C., Yang, T., Yang, J., 2022. Image recognition of wind turbine blade defects using attention-based MobileNetV1-YOLOv4 and transfer learning. *Sensors* 22, 6009. <https://doi.org/10.3390/s22166009>.

Zhou, K., Tang, J., 2021. Structural model updating using adaptive multi-response Gaussian process meta-modeling. *Mech. Syst. Signal Process.* 147, 107121. <https://doi.org/10.1016/j.jmssp.2020.107121>.

Zhou, K., Tang, J., 2021. Computational inference of vibratory system with incomplete modal information using parallel, interactive and adaptive Markov chains. *J. Sound Vib.* 511, 116331. <https://doi.org/10.1016/j.jsv.2021.116331>.

Zhou, K., Tang, J., 2021. Uncertainty quantification of mode shape variation utilizing multi-level multi-response Gaussian process. *J. Vib. Acoust.* 143. <https://doi.org/10.1115/1.4047700>.

Zhou, K., Wu, Z.Y., 2017. Strain gauge placement optimization for structural performance assessment. *Eng. Struct.* 141, 184–197. <https://doi.org/10.1016/j.engstruct.2017.03.031>.

Zhou, K., Wu, Z.Y., Yi, X.H., Zhu, D.P., Narayan, R., Zhao, J., 2017. Generic framework of sensor placement optimization for structural health modeling. *J. Comput. Civ. Eng.* 31, 04017018. [https://doi.org/10.1061/\(asce\)cp.1943-5487.0000662](https://doi.org/10.1061/(asce)cp.1943-5487.0000662).

Zhou, K., Enos, R., Zhang, D., Tang, J., 2022. Uncertainty analysis of curing-induced dimensional variability of composite structures utilizing physics-guided Gaussian process meta-modeling. *Compos. Struct.* 280, 114816. <https://doi.org/10.1016/j.compstruct.2021.114816>.